Proceedings of the Master's Programme
COGNITIVE NEUROSCIENCE

Characterizing Cognitive Defects of Myotonic Dystrophy Type 1 in a Dish: Insight From Induced Neurons

Lisa Rahm[1]

Supervisors: Renée H.L. Raaijmakers[1,2], C. Rosanne M. Ausems[1,2], Marina Hommersom[2], Derick G. Wansink[3], and Hans van Bokhoven[1,2]

Corresponding author: Lisa Rahm
E-mail: lisa.rahm@freenet.de

[1]Radboud University Nijmegen, Donders Institute for Brain, Cognition and Behaviour, The Netherlands
[2]Radboud University Medical Centre Nijmegen, Donders Institute for Brain, Cognition and Behaviour, The Netherlands
[3]Radboud Institute for Molecular Life Sciences, The Netherlands

Myotonic dystrophy type 1 (DM1) is an inherited autosomal dominant multisystemic disorder including symptoms in the central nervous system. Symptoms include cognitive and memory deficits, which seem to be caused by global synaptic dysfunction. In order to recapitulate the brain phenotype, we created neurons from induced pluripotent stem cells (iPSC) from DM1 patients, which was done by an imposed expression of the transcription factor neurogenin-2. From there, we performed immunocytochemistry and electrophysiological recordings of the neuronal activity. Reverse transcriptase quantitative polymerase chain reaction (RT-qPCR) experiments were performed to study gene expression of DM1 related genes. iPSC express less DM1 specific genes compared to adult myoblasts. We, furthermore, demonstrated that it is possible to differentiate iPSCs from DM1 patients into iNeurons that show DM1 disease markers, and we made a step toward unravelling the DM1 neuropathophysiology.

KEYWORDS Myotonic Dystrophy Type 1, neuromuscular disorder, induced neurons, immunocytochemistry, multi-electrode array analysis

Abbreviations

DM1 – Myotonic dystrophy type 1
CNS – Central nervous system
UTR – untranslated region
DMPK – Dystrophia Myotonica Protein Kinase
CTG – cytosine-thymine-guanine
CUG – cytosine-uracil-guanine
RNA – ribonucleic acid
GOF – gain-of-function
MBNL – muscleblind-like proteins
PKC – protein kinase C
CELF – CUG/Elav-like family
NFT – neurofibrillary tangles
MAPT – microtubule associated protein Tau
MRI – magnetic resonance imaging
GM – grey matter
WM – white matter
FISH – fluorescence in situ hybridization
CAG – cytosine-adenine-guanine

IF – immunofluorescence
NMDAR - N-methyl-D-aspartate receptor
LTP – long-term potentiation
iNeurons – induced neurons
hiPSC – human induced pluripotent stem cells
SCTC – Stem Cell Technology Centre
RT-qPCR – reverse transcriptase quantitative polymerase chain reaction
MIRS – Muscle Impairment Rating Scale
RIMLS – Radboud Institute for Molecular Life Science
STD – standard deviation
HKG – housekeeping genes
WP – well plate
MTG – Matrigel
PLO – Poly-L-Ornithine
(O/N) – overnight
hNT3 – human Neurotrophin-3
hBDNF – human Brain-derived Neurotrophic Factor
Ara-C – Cytosine β-D-arabinofuranoside
FBS – Foetal bovine serum
PBS - Phosphate-buffered saline
PFA – paraformaldehyde
RT – room temperature
Ac:Me – Aceton-Methanol
MAP2 – Microtubule-associated protein 2
MEA – multi-electrode array
PCR – polymerase chain reaction
GLT1 - Glutamate transporter 1
SP-PCR - small pool PCR
TP-PCR – triplet primed PCR
SRY – Sex Determining Region

Myotonic dystrophy type 1 (DM1) is a multi-systemic neuromuscular disorder with an estimated prevalence of at least 1 in 8,000 (Caillet-Boudin et al., 2014; Longman, 2006). This disorder affects several organs in the body, such as skeletal and smooth muscles, the heart, the eyes, and the central nervous system (CNS). This leads to symptoms such as myotonia (the delayed relaxation after voluntary muscular contraction), muscle weakness and wasting, arrythmias and conduction defects, as well as breathing difficulties, and cataracts (Dhaenens et al., 2011; Wenninger, Montagnese, & Schoser, 2018). DM1 is known for its typical symptoms such as myotonia and muscle wasting, but it is also accompanied by cognitive impairments such as executive dysfunction, visuospatial deficits and abnormal social cognition (Caillet-Boudin et al., 2014; Dhaenens et al., 2011; Hernández-Hernández et al., 2013; Suenaga et al., 2012). Executive function is important for daily life, it is involved in planning, time management and solving problems. Visuospatial skills are also required in daily life. With a deficit in this domain, difficulties can range from identifying and processing simple visual stimuli, up to identifying faces or whole scenes (Scott & Schoenberg, 2006). Abnormal social cognition is defined by the difficulties in processing, decoding and encoding, storing, and applying information about social situations or other people (Beer & Ochsner, 2006). These deficits are said to be caused by abnormal neuronal morphology and malfunctioning synapses.

DMI is caused by an autosomal dominant gene mutation in the 3' untranslated region (UTR) of the Dystrophia Myotonica Protein Kinase (DMPK) gene, which is located on chromosome 19q13.32. The mutation is an expanded repeat of the base-pair triplet sequence cytosine-thymine-guanine (CTG). Healthy individuals have a repeat sequence ranging from 5 to 37 and do not show disease burden. However, a repeat of 50-1000 CTG-triplets, is associated with a wide range of mild to severe DM1 symptoms. Mild symptoms include facial and distal muscle

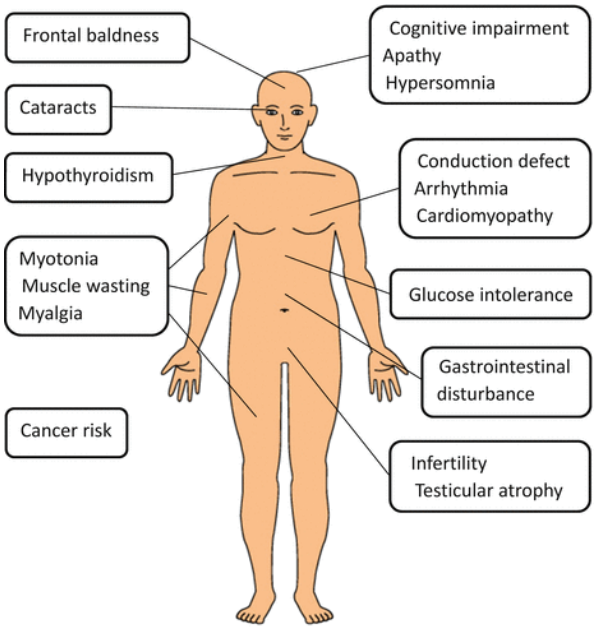

Figure 1. Affected body parts in DM1 patients. Reprinted from Nakamori & Takahashi (2016).

weakness, and severe symptoms include additional cognitive impairment and other extra muscular symptoms (Wenninger et al., 2018). The childhood/juvenile phenotype is associated with an early onset and typically has >800 CTG-repeat. The congenital form is the most severe with usually >1000 CTG-repeat (Wenninger et al., 2018). The repeat length is not only critically linked to disease severity and age of onset, but also shows genetic anticipation: the tendency to grow over time in the patient due to somatic instability (Caillet-Boudin et al., 2014; Morales et al., 2012; Yum, Wang, & Kalsotra, 2017) and to increase in size from one generation to the next. This results in increased disease burden (Dhaenens et al., 2008; Gomes-Pereira et al., 2007; Morales et al., 2012). For DM1, somatic instability means that the CTG repeat length differs between tissue types (e.g., longer repeats have been found in muscle and the brain compared to leukocytes) (Jinnai et al., 2013).

The disease pathogenesis of DM1 reveals that the corresponding phenotype appears to be regulated mainly by a deleterious gain-of-function (GOF) caused by the expanded DMPK transcripts. These transcripts form secondary hairpin-like RNA structures that bind to and sequester muscleblind-like proteins (MBNL) into ribonuclear inclusions, also known as RNA foci (André, van Cruchten, Willemse, & Wansink, 2019). Furthermore, cytosine-uracil-guanine (CUG) expansions in the 3'-UTR of the DMPK mRNA are activated by the protein kinase C (PKC) pathway which results in phosphorylation of CUG/Elav-like family (CELF1) proteins. This hyperphosphorylation causes a stabilization of the protein and results in its upregulation (Gallo & Spickett, 2010). Together with MBNL proteins, CELF proteins are responsible for the regulation of splicing mechanisms, however, the RNA toxicity caused by CUG-repeat results in aberrant splicing patterns – therefore, DM1 is defined as spliceopathy (Hernández-Hernández et al., 2013). Muscle weakness and loss are results of these aberrant splicing patterns and several mis-splicing defects have also been reported to occur in the DM1 brain. However, the mis-splicing in neuropathophysiology is not currently understood. In several recent studies, DM1 has also been described as a RNAopathy due to its toxic RNA GOF, and as a tauopathy because neurofibrillary tangles (NFT) have been found in the brain of DM1 patients (Dhaenens et al., 2008; Dahenens et al., 2011). The group of tauopathies encompasses several neurodegenerative diseases which are all characterized by intraneuronal protein aggregates of the microtubule-associated protein Tau (MAPT) in the amygdala, hippocampus, entorhinal cortex, and temporal cortex (Caillet-Boudin et al., 2014; Dhaenens et al., 2011; Hernández-Hernández et al., 2013). Our knowledge of the CNS-related symptoms in DM1 patients is based on MRI studies, post-mortem brain material of DM1 patients, and on DM1 mouse models.

MRI studies have been conducted to investigate the DM1 brain phenotype in terms of structural brain abnormalities, such as loss of grey matter (GM) regions and white matter (WM) regions (Caillet-Boudin et al., 2014; Hamilton et al., 2018; Van der Plas et al., 2019). Global cerebral atrophy and loss of cortical GM has been found in brain regions involved in cognitive functioning, attention, memory and visuospatial functioning (Caillet-Boudin et al., 2014; Ramon-Duaso et al., 2020). Lesions in WM temporal lobes are a very prominent phenotype in the DM1 brain, and are even more distinctive than GM lesions (Caillet-Boudin et al., 2014).

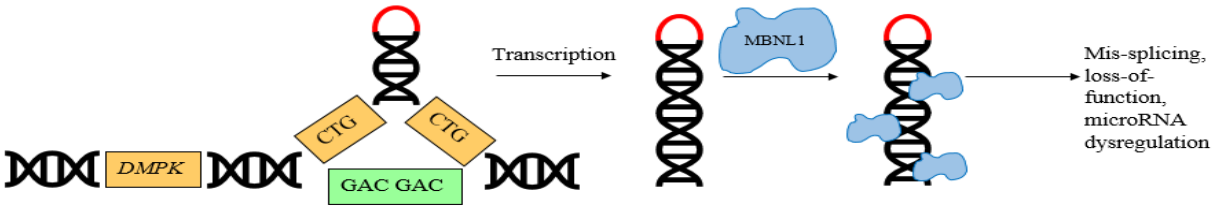

Figure 2. Expanded CTG triplets in 3'UTR of DMPK are transcribed to r(CUG)exp, forming secondary hairpin-like structures. Members of the MBNL family such as MBNL1 are sequestered into ribonuclear inclusions which cause a loss-of-function, mRNA mis-splicing and microRNA dysregulation (Udd & Krahe, 2012).

Post-mortem brain material of DM1 patients has also been studied, however, the difficulty here is that active processes cannot be studied. Nonetheless, we can still gain information about repeat size in different tissue types. Jiang, Mankodi, Swanson, Moxley, and Thornton (2004) performed fluorescence in situ hybridization (FISH) with a (CAG)6 probe of brain sections and found nuclear RNA foci in every patient. Each (CAG)6 probe is labelled with a fluorescent dye and to become visible, a certain threshold needs to be reached. The number of foci per neuron ranged from 1 up to 15 foci.). However, due to technical limitations in microscopy (Sanderson, Smith, Parker, & Bootman, 2014), a lot less RNA foci have been found in patients with a short repeat and a mild phenotype (Jiang et al., 2004).

Braz and colleagues (2018) reported that in DM1 mouse models pre- and postsynaptic events are involved in the dysregulated disease mechanism. Those events reflect global synaptic dysfunction, which then causes cognitive and memory deficits. More precisely they state that in DMSXL mice, transgenic mice carrying the human DM1 locus with an (CTG)>1000, impaired short-term plasticity was found in the pre-synapse, which was mostly caused by a decrease in the paired-pulse facilitation (Braz, Acquaire, Gourdon, & Gomes-Pereira, 2018; Hernández-Hernández et al., 2013). Charizanis et al. (2012) reported that MBNL1 and MBNL2 are the two major MBNL proteins that are expressed in adult tissue, and that MBNL2 appears to be the protein that is most dysregulated in the CNS in DM1 patients (Charizanis et al., 2012; Goodwin et al., 2015). Furthermore, in Mbnl2 knockout mice (Mbnl2ΔE2/ΔE2) they found Mbnl2 mostly in the nucleus of neurons in the hippocampal structure. Mbnl2ΔE2/ΔE2 mice showed a deficit in spatial reference memory. A loss of expressed Mbnl1 led to a decrease in synaptic N-methyl-D-aspartate receptor (NMDAR) activity, impaired long-term potentiation (LTP) and deficits in memory and learning (Charizanis et al., 2012). Additionally, splicing effects were also investigated and Mbnl2 was found to be essential in splicing regulation during brain development (Table S1) (Charizanis et al., 2012). The Mbnl2 knockout mouse model seemed to (at least partially) reproduce the brain pathology found in the human DM1 brain (Caillet-Boudin et al., 2014; Charizanis et al., 2012).

Aforementioned research on MRI, post-mortem material, and mouse models provides us with results about the DM1 brain structure to further unravel its pathological mechanisms. Nonetheless, these three ways to study the disease are not ideal. MRI investigations are limited by real-time resolution because a scan for the whole brain takes 2 to 3 minutes, which makes it difficult to see certain processes. A limitation of post-mortem material is that no active processes can be investigated, and tissue degrades. While mouse models mimic the disease and disease related behaviour to a certain extent, it would be helpful to study pathological mechanisms on living human DM1 material.

Therefore, the aim of this study is to develop a cell-based model by generating induced neurons (iNeurons) from human derived induced pluripotent stem cells (hiPSCs) of two DM1 patients. These derived iNeurons will then be compared with healthy iNeurons in terms of their morphology, electrophysiological profile and DM1 specific phenotypes such as RNA foci and (mis-) splicing.

Methods

The Stem Cell Technology Center (SCTC) at the Radboudumc created two iPSC lines from fibroblasts of two DM1 patients (Table 1). These fibroblasts were reprogrammed with lentiviral vectors containing the genes OCT4, SOX2, KLF4 and c-MYC (Elegheert et al., 2018). Gene expression profiles of stem cell markers were examined by RT-qPCR, in which an upregulation of SOX2, LIN28, NANOG and DNMT3B was found compared to parental fibroblasts of P1 and P2 (Fig. S1 and S2). Furthermore, cells were tested on protein expression of stem cell markers via immunocytochemistry. The undifferentiated iPSC clones were stained for the nuclear markers NANOG and OCT4 and surface antigens SSEA4 and TRA-81 (Fig. S3 and S4).

For having a better estimation of the repeat length of the P2, northern blotting was performed by the Department of Cell biology at Radboud Institute for Molecular Life Science (RIMLS) with 10µg RNA. The result of

Table 1.

Clinical and Genetic Data of Included Participants, unaffected control; DM1, DM1 patient; MIRS, Muscle Impairment Rating Scale (ranging from 1-5, where 1 indicates mild symptoms and 5 indicates severe symptoms); M, male; F, female; NA, not applicable; Fbr, fibroblast; Per., pericyte; TP-PCR, Triplet-primed PCR. P1, P2 and C2 are fibroblast-derived iPSCs, P3 and C1 are pericyte-derived iPSCs.

	Sex (M/F)	Disease (CONT/DM1)	MIRS	Repeat Length at Diagnosis (No. of Triplets)	Origin of parental cells	Repeat Length by TP-PCR (No. of Triplets)	Age at Biopsy (years)
P1	M	DM1	2	64-77 (in blood)	Fbr.	87-97 (in iPSC)	64
P2	F	DM1	4	> 150 (in blood)	Fbr.	> 150 (in iPSC)	35
P3	M	DM1	5	120 < N < 1000	Per.	NA	46
C1	M	CONT	NA	NA	Per.	NA	45
C2	M	CONT	NA	NA	Fbr.	NA	NA

the northern blot was inconclusive, and we were not able to get an estimate of the repeat length in the iPSCs. Triplet repeat primed PCR (TP-PCR) with 40ng DNA was performed by Genome Diagnostics at Radboudumc (Leferink et al., 2019). iPSC samples of P1 and P2 from different passages were taken along. The results of the TP-PCR show that the repeat length of P1 is between 87 and 97, in iPSCs. The repeat length of P2, in iPSCs, is still above 150 and out of determination range of the TP-PCR. Small-pool PCR was used to determine repeat length of P3 and C1, confirming that C1 is a healthy individual, while iPSCs from P3 contain a repeat larger than 1500 (unpublished data), (Gomes-Pereira, Bidichandani, & Monckton, 2004).

Assessment of gene expression levels in iPSCs

RNA was extracted (NucleoSpin, Macherey-Nagel) and cDNA synthesis by random hexamers (iScript) was performed in order to gain more information about expression levels of genes of interest by RT-qPCR. DM1 related genes (MBNL1-3, DMPK e1-2, DMPK e15 3'), iPSC-specific genes (TBP e3, HPRT1 e7-9), and housekeeping genes (GUSB e11-12, GAPDH e1) were used. To optimize the primers, every gene was tested in a dilution range from 1:20 to 1:320 with contamination controls: milliQ (MQ, nuclease-free water) and RT- (cDNA synthesis excluding reverse transcriptase enzyme) as a control to guarantee that the cDNA is free from genomic DNA. All primer and cDNA mixes were pipetted in duplo to measure their standard deviation (STD). For the later RT-qPCR experiment we used 1.667 ng/µL cDNA because the Ct values were most reliable and in the preferred range below 30. Furthermore, gene expression levels of the genes of interest were measured for C25 adult myoblasts as a comparison of MBNL1-3. Additionally, the cells from P1, P2, P3 and C1 were taken along, as a comparison for MBNL and DMPK expression.

Generation of Tet-On 3G and NGN2 stable lines, a pre-step for the differentiation of hiPSCs into iNeurons

The generation of the stable lines with Tet-On 3G and NGN2 was performed according to the protocol published by Frega et al. (2017) however, we used 12-well plates (12WP) coated with 1:15 MTG (0.53 – 0.67 mg/mL), instead of a geltrex-coated 12WP. Furthermore, instead of accutase (Sigma) we used TryplE Select 1X for detachment and Essential 8 flex medium was supplemented with 1 mg/mL primocin (InvivoGen). For counting the cells, the following formula was used to calculate the total amount of cells per milliliter:

$$\frac{\text{no. of counted cells}}{\text{no. of counted chambers}} \times \text{volume of orig. cell suspension in µL} \times 10{,}000 = \text{cells/mL}$$

After counting, the volume for 50,000 cells was calculated and then placed with a sufficient amount of media in a well of a 12WP. The

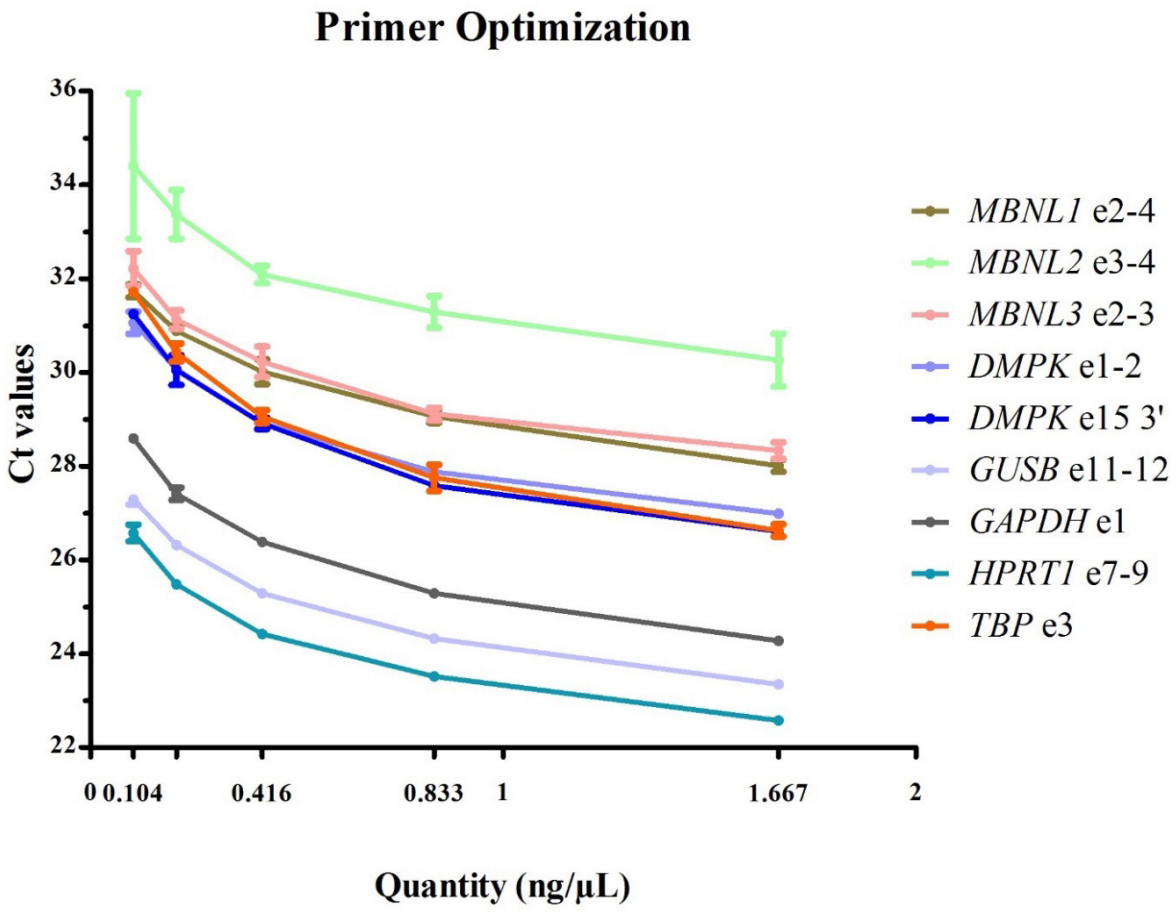

Figure 3. Standard Curve of primer optimization. Primer pairs were tested on iPSC line of P1 on Genes of Interest (GoI): MBNL1 e2-4, MBNL2 e3-4, MBNL3 e2-3, DMPK e1-2, DMPK e15 3', Housekeeping Genes (HKG): GUSB e11, GAPDH e1, and iPSC specific Genes: HPRT1 e7-9, TBP e3. Used quantities were 0.104ng/µL, 0.208ng/µL, 0.416ng/µL, 0.833ng/µL and 1.667ng/µL. Therefore, the pictured dilutions are 1:320, 1:160, 1:80, 1:40 and 1:20. The Ct values are depicted with an error bar, indicating the deviation between the samples which were pipetted derived in duplo.

next day the iPSCs are transduced with the Tet-On 3G and NGN2 lentiviral constructs. The transfer vector that was used for the Tet-On 3G lentivirus is pLv.EF1a_TET3g.IRES.Neo; This vector, controlled by the EF-1a promoter region, encodes a Tet-On trans-activator and is resistant to neomycin (also known as G418). The transfer vector which was used for the NGN2 lentivirus is pLv.TRE3G.mNeurog2.Puro: The Tet-controlled promoter causes encoding of murine neurogenin-2 and the puromycin resistance gene. Both viruses were used in the concentrated form with the following packaging vectors: psPAX2 and pMD2.G.

We used different amounts of the lentiviral constructs compared to the ones by Frega et al. (2017) because we transduced the iPSCs with the third generation of lentiviruses. The concentrations which have been used to select Tet-On 3G-/NGN2-positive cells also had to be adjusted, due to the same reason. Important is that from day five on, a basal concentration of the antibiotics was added as soon as the media was refreshed. The selection period must be adapted to the state of the cells and can take longer.

Differentiation of Tet-On 3G- and NGN2-positive hiPSC lines into iNeurons

To use Tet-On 3G- and NGN2-positive iPSCs for the differentiation, plates need to be coated such that the coating can solidify and cover the surface of the wells. We used Poly L-Ornithine (PLO) diluted in 50 mM borate buffer (50 µg/mL) which was then filtered and added to each well. The plates were placed for three hours in a humidified 37 °C

Table 2.

Lentiviral Transductions Concentrations of lentiviral constructs. Transduction number 4 and 5 were positive controls.

Transduction number	Tet-On 3G	NGN2
1	1µL	1µL
2	2µL	4µL
3	4µL	4µL
4	1µL	0µL
5	0µL	1µL

incubator with an atmosphere of 5% CO2. For the second part of the coating, human laminin [20 µg/mL, BioLamina] was diluted in cold Dulbecco's Modified Eagle Medium: Nutrient Mixture F-12 (DMEM/F12, gibco) by using cold pipet tips. Afterwards the plate was sealed with parafilm (Bemis) and incubated overnight (O/N) at 4 ºC.

The subsequent day, iPSCs were made single cell, and doxycycline (4 µg/mL, Sigma) was added to induce expression of NGN2. For the day after plating the iPSCs as single cells no adjustments were made to the protocol by Frega et al. (2017). On day two of the differentiation, rat astrocytes were added to each well in a 1:1 ratio. For day three, adaptations were made for the supplements added to the neurobasal medium (gibco). It was supplemented with primocin (1:500 concentration), doxycycline (4 µg/mL), B-27 supplement 100X (1:50, gibco), glutamaxsupplement 100X (1:100 concentration, gibco), human Neurotrophin-3 (10 ng/mL) (hNT-3, Primokine), human Brain-derived Neurotrophic Factor (10 ng/mL) (hBDNF, Primokine). Furthermore, Cytosine β-D-arabinofuranoside (2 µM) (Ara-C, Sigma). Ara-C was added to form a pure neuronal and astrocyte culture as it has an inhibiting function on astrocyte proliferation and kills remaining iPSC . From day six until day eight, around 50% of the medium per well is refreshed every second day. The required medium is the same as the one prepared for the day after adding the rat astrocytes, except that from day six until day eight no Ara-C was added. The first test differentiation stopped at this point and immunocytochemistry was performed. The results can be found in the results section under 'iNeuron characterization'.

From day eight onwards, around 50% of the spent neurobasal medium is refreshed every second day and the medium is supplemented with 2.5% Fetal bovine serum (FBS, Sigma) in order to sustain the astrocytes.

Immunofluorescence and Immunocytochemistry

DM1 disease markers in iPSC.

iPSCs were grown on coverslips which were coated with 1:50 phenol-red free growth factor reduced Matrigel (0.16 – 0.2 mg/mL, depending on the concentration in the bottle) [MTG, Corning] in 1x Phosphate-buffered saline (PBS). Protocols for RNA FISH (Stellaris kit, Biosearch Technologies), MBNL1, and FISH + MBNL1 were used.

For FISH, only our adjustments of the Stellaris protocol are listed in the following part. On day one for FISH, the cells were washed with 1x PBS and fixated in 1 mL 4% paraformaldehyde (PFA) for 10 min at room temperature (RT). To hybridize the cells, we applied 25 µL Hybridization Buffer

Table 3.

Concentrations of Antibiotics during Selection Period.

Day	Concentration neomycin (G418, Sigma)	Concentration puromycin (Sigma)
1	25 µg/mL	0.5 µg/mL
2	50 µg/mL	0.5 µg/mL
3	100 µg/mL	1 µg/mL
4	200 µg/mL	2 µg/mL
5 and later	50 µg/mL	0.5 µg/mL

per coverslip. For day two we followed the Stellaris protocol.

The protocol for the MBNL1 staining is as follows: On day one, the cells were washed with prewarmed 1x PBS and then fixated in -20 ºC cold Acetone-Methanol (Ac:Me, 1:1) for 10 min. Afterwards, cells were washed 3x 5 min with 1x PBS and then permeabilized 10 min in 0.2% Triton. After permeabilization, coverslips were placed in blocking buffer for 1 hour at RT then incubated in blocking buffer and MBNL1 (1:10, 50µL per coverslip) at 4 ºC O/N. On day 2, the cells were washed 3x 5 min in 1x PBS at RT and before incubation with 4 mg/mL goat-anti-mouse (Invitrogen) and 100 ng/mL DAPI for 1 hour in the dark at RT. Cells were then washed 3x 5min with 1x PBS, then dipped in MQ and mounted on an empty object slide.

For the combined staining of RNA FISH and MBNL1, we followed the Stellaris protocol with our adjustments (day 1). On day two, after the cells were incubated in Wash Buffer B, they were fixed in ice-cold Ac:Me and incubated for 10 min in the dark at -20 ºC. Afterwards, they were washed 3x 5 min in 1x PBS and then incubated 1 hour at RT in blocking buffer. Then, they were incubated in blocking buffer and MBNL1 (1:10, 50 µL per coverslip) at 4 ºC O/N. On day three, we followed the MBNL1 protocol for day two.

Fluorescent images of iPSC were acquired using a Leica DMI6000B microscope with x20 and x63 objectives (Fig. 8).

iNeuron characterization

The iPSCs were seeded for differentiation to iNeurons on glass coverslips coated with PLO in borate buffer and human laminin coating and kept on the coverslips for the desired time. Coated coverslips were washed 3x 5 min with ice-cold 1xPBS and fixated in 4% PFA for 15 min at RT and afterwards washed 3x 5 min with 1x PBS. The plates were stored at 4 ºC until the next day. On day one, the coverslips were permeabilized with 0.2% Triton for 10 min at RT, then washed 3x 5min with 1x PBS. The neurons were incubated with blocking buffer (5% goat serum in 1x PBS, 1:20) for 1 hour at RT. Primary antibodies, Pan-Axonal Neurofilament Marker (mouse monoclonal, BioLegend), Microtubule-associated protein 2 (MAP2, rabbit polyclonal, Abcam), and Synapsin 1/2 (guinea pig polyclonal, Synaptic systems), were diluted in blocking buffer and were applied onto the coverslips and incubated O/N at 4 ºC in a box containing moist tissues. On day two, the coverslips were washed 3x 5 min with 1x PBS and secondary antibodies, Goat anti-Mouse Alexa Fluor 488 (Ab-M34-03, Invitrogen), Goat anti-Rabbit Alexa Fluor 568 (Invitrogen), and Goat anti-Guinea Pig Alexa Fluor 647 (Ab-G50-01, Invitrogen), diluted in blocking buffer were applied to the coverslips and incubated 1 hour at RT in the dark. Afterwards, coverslips were washed 3x 5 min in 1x PBS, then Hoechst 33342 (10 mg/mL solution in water, Invitrogen) was added and incubated for 10 min at RT. Neurons were washed again 3x 5 min with 1x PBS and mounted on an empty object slide.

Images were acquired with a Zeiss Axio Imager Z1 using a x40 objective (Fig. 9) and with a Zeiss LSM880 confocal microscope with 405 and 561 nm diode lasers, argon (458, 488, 514 nm) and a 633 nm laser using a x20 objective (Fig. 10).

Establishment of electrophysiological profile of iNeurons

For the acquisition of the electrophysiological profile of the iNeurons derived from the DM1 patients and a healthy control, we used the multi-electrode array (MEA). Here, we performed the differentiation of the iPSCs to iNeurons in a 24WP for Multiwell-MEA-System (multichannel* systems, MCS GmbH). In each of the 24 wells, 12 gold electrodes with a distance of 300 µm and a dimeter of 30 µm are placed.

We plated iPSCs from P1, P2 and a wild-type iPSC line (further referred as C2) and differentiated them according to the protocol. Basal recordings of each 10 minutes of the iNeurons were performed on differentiation day (days in vitro, DIV) 14, 21 and 28. The software used for the recordings was Multi-well-Screen (multichannel* systems, MCS GmbH).

PCR for Y chromosome check

After we performed the previously mentioned experiments, we realized that the results of these experiments were not matching with

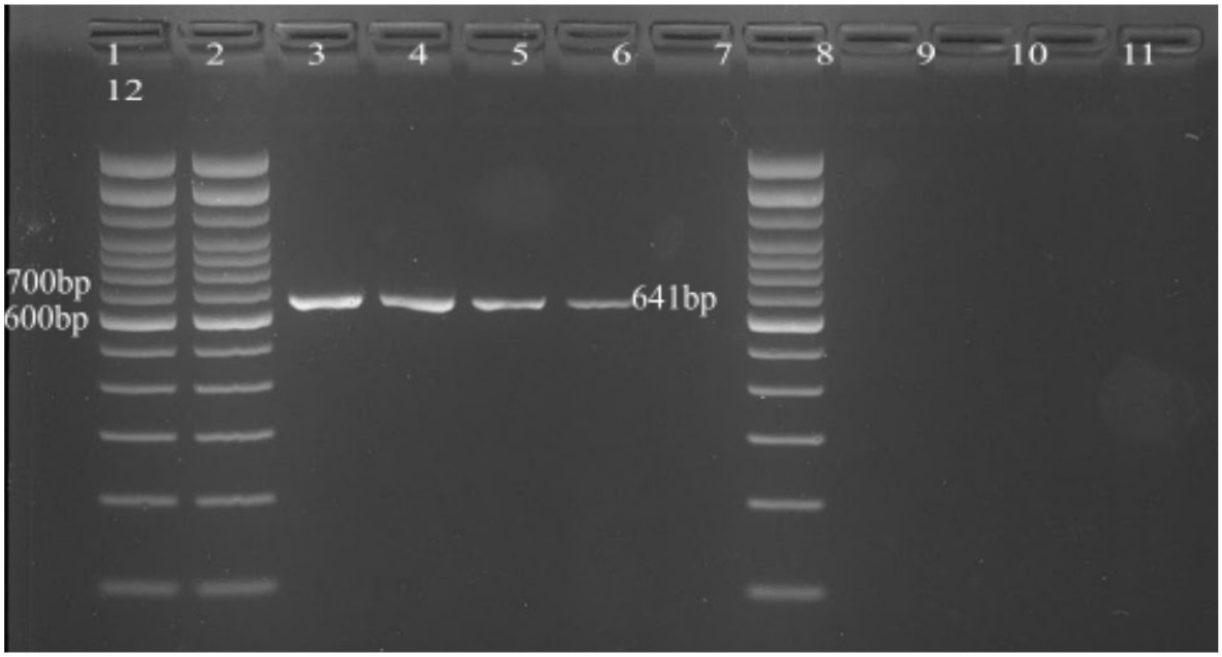

Figure 4. Gel electrophoresis of PCR products for detection of the SRY gene. The first two columns show a 100bp ladder as reference, column 3 to 5 show DNA samples of P1which was supposed to be female but is male. Column 6 is a positive control (male sample). Column 7 is empty. Column 8 shows again the 100bp ladder. Columns 9 to 11 show the samples of P2, which was supposed to be male, but is female. Column 12 shows a negative control (female sample).

our expectations. Therefore, we performed a Y chromosome check with PCR, to distinguish the male from the female sample. We designed an oligonucleotide primer pair for the SRY (Sex-Determining Region Y) gene (exon 1) with the following sequences for forward 5′ - CTG CTA TGT TAA GCG TAT TC - 3′ and for reverse 5′ – AGC ATC TAG GTA GGT CTT TG – 3′. The expected band size for the product is 641 base pairs (bp). As a basis we used the protocol by Settin, Elsobky, Hammad, and Al-Era (2008). We used 40 ng of DNA sample per reaction, which has been isolated with the QIAamp DNA Blood Mini Kit (QIAGEN) and measured with the Qubit fluorometer (Invitrogen). Each reaction had a total volume of 25 µL, with 5 µL Q5 Buffer (New England BioLabs), 0.5 µL dNTPs, each 1.25µL of forward and reverse primer, 0.25 µL Q5 enzyme (New England BioLabs) and MQ up to the 25 µL total volume. The PCR reactions have been performed for 3 samples for P1 and for 3 samples for P2 (two for each at different passages during iPSC stage and one at the stage which has been used for iNeurons differentiation). Additionally, a positive control (male) and a negative control (female) have been added. The PCR reactions were carried out in a thermal cycler (Applied Biosystems) according to the protocol by Settin et al. (2008). All amplified PCR products were separated by gel electrophoresis in a 2% agarose gel, stained with ethidium bromide (10 mg/mL, Invitrogen). The applied voltage was 100 V for 90-110 minutes.

Results

PCR for Y chromosome check

The gel electrophoresis of the PCR products of P1, P2 and positive and negative control samples show that P1 who was supposed to be female shows a band for the SRY gene at the expected level of 641 bp. P2 who was supposed to be male does not show a band for the SRY gene. This experiment clearly shows that the samples of P1 and P2 were switched around. The result can be found in Figure 4. We included for each patient three iPSC samples from different time points, in order to find at what time point the samples were switched. As a reference we included a 100 bp ladder. For the further results, P1 is male and P2 is female.

Assessment of gene expression

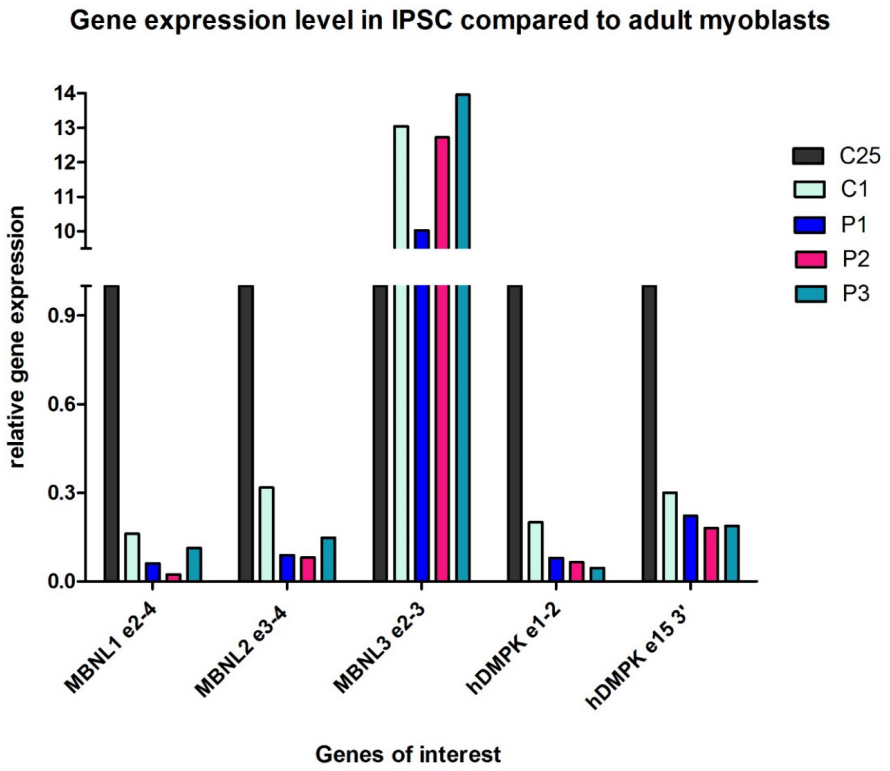

Figure 5. Relative Gene Expression of Genes of Interest (GoI). GoI were tested on two patient iPSC lines which were fibroblast-derived and lentiviral transduced (P1 [repeat in iPSC: ~87-97], P2 [repeat in iPSC > 150]), on two iPSC lines which were pericyte-derived and lentiviral transduced (P3 [repeat > 1500, determined by SP-PCR], C1) and on C25, adult myoblast as a reference for MBNL1-3 expression.

levels in iPSCs from DM1 patients

The results of the RT-qPCR for assessing relative gene expression levels show that the genes of interest MBNL1, MBNL2, DMPK e1-2, and DMPK e15 3' are expressed a 3- to 6-fold lower in iPSC derived from P1, P2, P3 and C1, relative to C25. MBNL3 is expressed 10- to 13-times higher compared to C25. Even the control (C1) showed slightly higher gene expression levels of MBNL1, MBNL2, DMPK e1-2 and DMPK e15 3'. The samples for this RT-qPCR are pipetted in triplo, the whole experiment was performed in n = 1.

Differentiation of Tet-On 3G- and NGN2-positive hiPSC lines into iNeurons

We successfully differentiated Tet-On 3G- and NGN2-positive iPSCs into iNeurons. We first used three different cell densities (17,500; 20,000; 22,500) in order to have a range and see what works best. The cell density of 17,500 cells per well in a 24WP was sufficient for the cells to survive and differentiate. Already from day two on, the shape of the cells changed from small round to a more neuron-typical shape. A few days after starting the differentiation, the cells looked like neurons and started spreading. However, Ara-C, which was added to the iNeuron's medium, was not as efficient as expected. This can be seen on the living iPSCs that remained in the wells (see Fig. 6 and 7, Day 5 and Day 6). Figures 6 and 7 show a day-by-day timeline of the development of iPSCs to iNeurons.

Immunofluorescence and immunocytochemistry

DM1 disease markers in iPSC.

To visualize DM1 disease markers, immunofluorescence staining was performed for the iPSCs of P1 and P2. The immunofluorescence staining (Fig. 8, A & B) revealed that in the iPSCs of P1 at an early passage, no intranuclear foci could be detected. The same

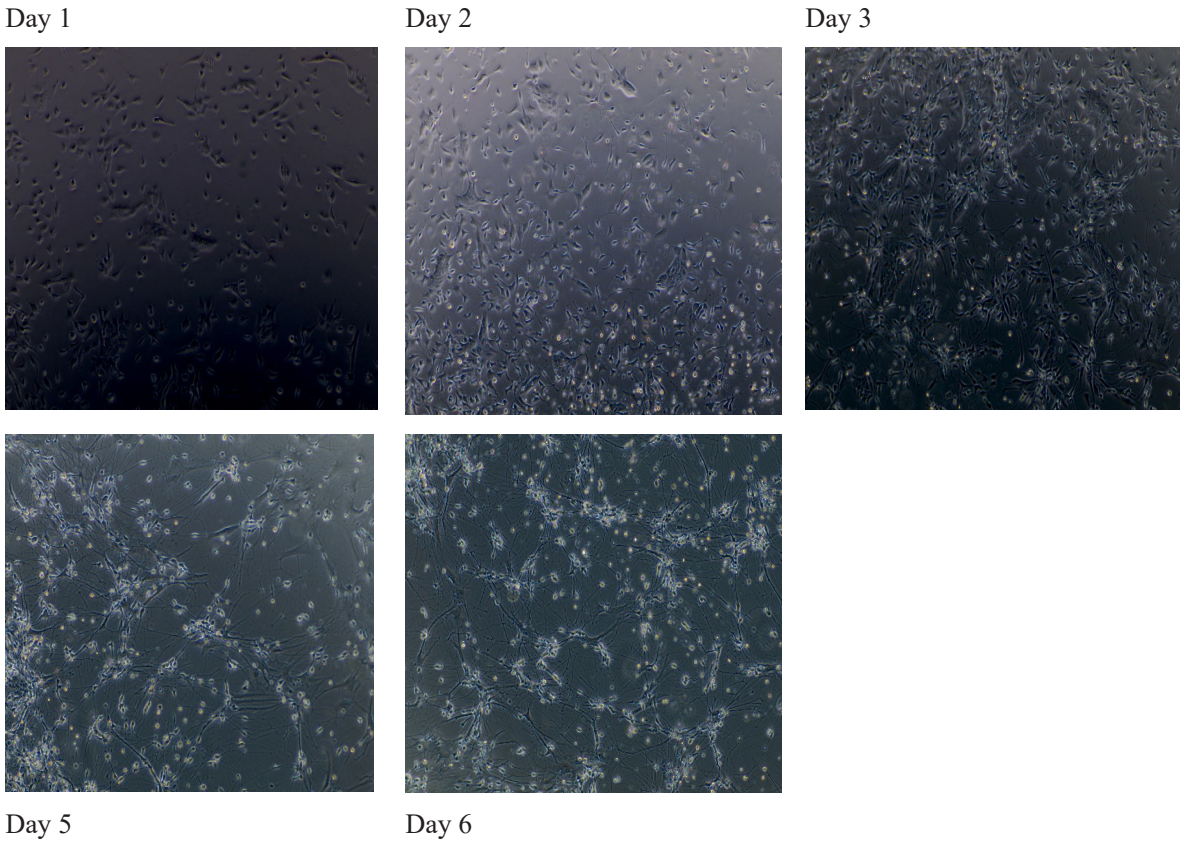

Figure 6. Day 1 until Day 6 of Differentiation of iPSC to iNeurons, of P1. The images show a cell density of 17,500 cells.

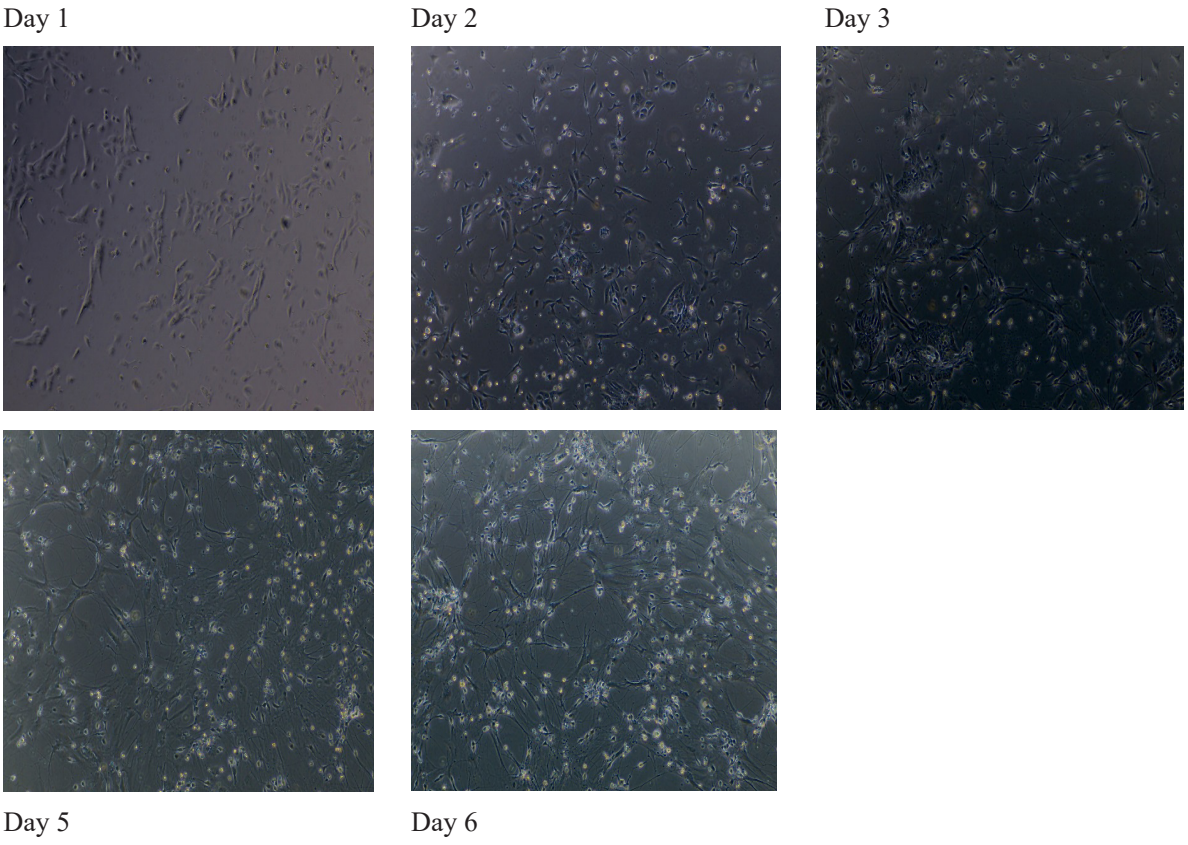

Figure 7. Day 1 until Day 6 of Differentiation of iPSC to iNeurons, of P2. The images show a cell density of 17,500 cells.

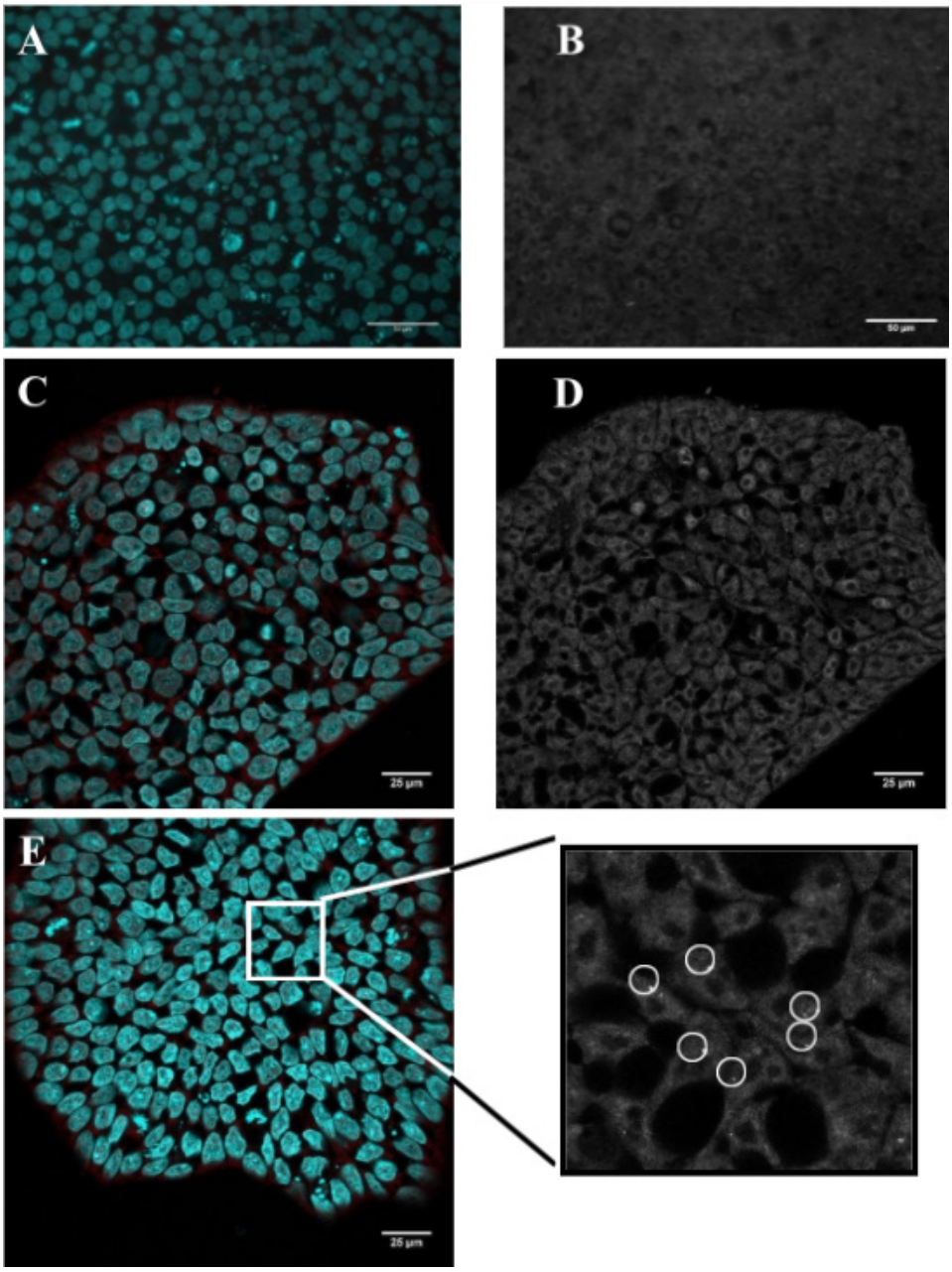

Figure 8. Images A and B show immunofluorescence staining on iPSCs of P1 for FISH + MBNL1 and DAPI, where image B shows a greyscale image of the (CAG)6 probe. Images C and D show the immunofluorescence staining for FISH on iPSCs of P1, where image D shows a greyscale image of the (CAG)6 probe. Image E shows immunofluorescence staining for FISH on iPSCs of P2, with a zoom-in in greyscales of the (CAG)6 probe to better visualize RNA foci. Images A and B were acquired with a Leica DMI6000B microscope. Images A and B were acquired with an x63 objective. The scale bar indicates a length of 50µM. Images C, D and E were acquired with a Zeiss LSM880 confocal microscope with 405 and 561 nm diode lasers, argon (458, 488, 514 nm) and a 633 nm laser using a x20 objective. Here the scale bar indicates a length of 25µM.

holds for MBNL1, we did not get a signal. Figure 8 C & D shows the FISH immunofluorescence (without MBNL1) of P1 at a later passage and Figure 8 E shows the FISH immunofluorescence (also without MBNL1) of P2. As it can be seen in Figure 8 C and D, no RNA foci were visible. However, in the iPSC of P2 we found intranuclear RNA foci (Fig. 8 E).

iNeuron characterization.

Immunocytochemistry was performed on iNeurons of P1 and P2 on DIV 6, and on mature iNeurons on DIV 49. The results of the immu-

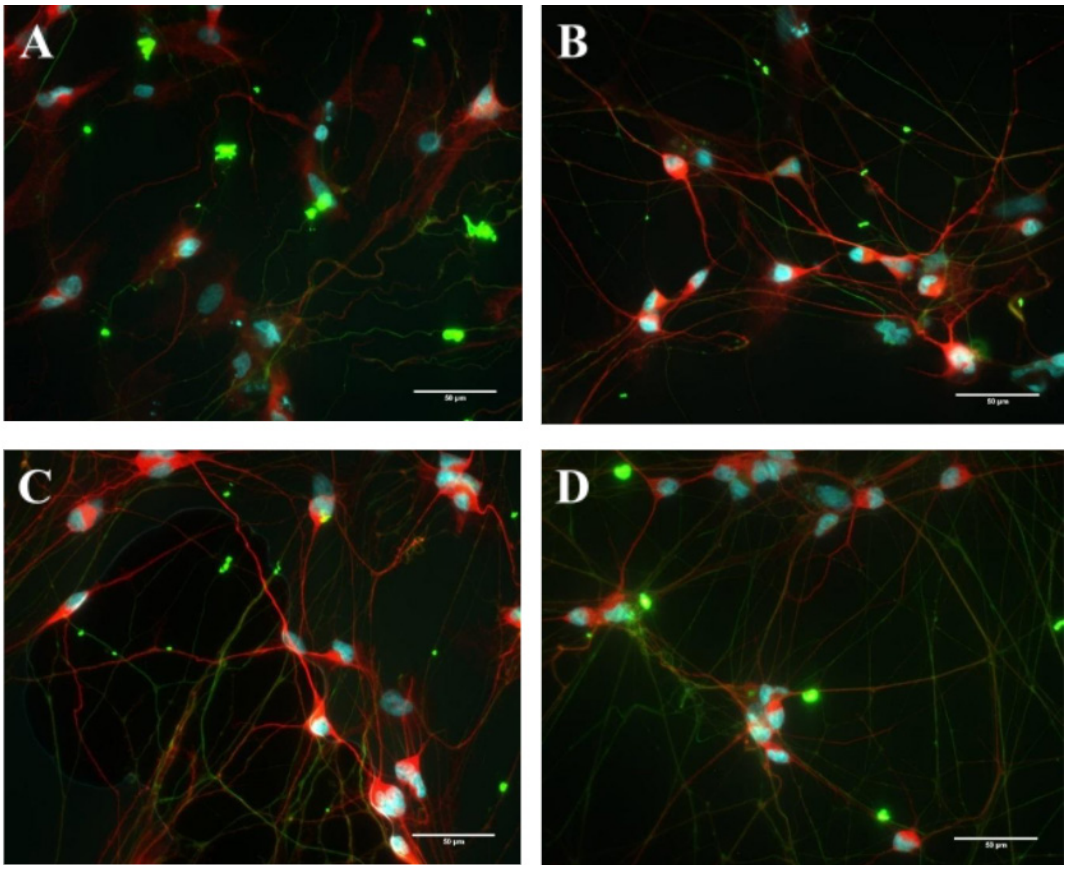

Figure 9. Immunocytochemistry of test-differentiated iNeurons at DIV6 and passage 3 from P1 and P2. A and B refer to P1 and C and D refer to P2. The antibodies used are Pan-Axonal Neurofilament Marker (mouse monoclonal, BioLegend) in green for the axons, Microtubule-associated protein 2 (MAP2, rabbit polyclonal, Abcam) in red for the dendrites, and Hoechst 33342 (10mg/mL solution in water, Invitrogen) in cyan for the nuclei. Images were acquired with a Zeiss Axio Imager Z1 microscope, using an x40 objective. The scale bar indicates a length of 50µM.

nocytochemistry performed on iNeurons of P1 and P2 on DIV 6 (Fig. 9) showed that, axons and dendrites were present and connections between neurons were made. The images in Figure 8 confirm that the differentiation of Tet-On 3G- and NGN2-positive iPSCs of DM1 patients was successful. We stained the iNeurons (DIV6) with antibodies for the axons, the dendrites, the synapses and the nuclei. For the synapses, however, we did not get a signal. This was due to their immature state after only 6 days in vitro. iNeurons get more mature between DIV14 and DIV21. After three weeks in culture, these iNeurons can be defined as mature (Cullen, Gilroy, Irons, & La Placa, 2010).

The results of immunocytochemistry performed on DIV49 show that iNeurons from DM1 patients are able to become mature and to survive the 7 weeks. For this staining we took healthy control (C2) iNeurons along in order to compare the healthy iNeurons with DM1 diseased iNeurons. In Figure 10, the iNeurons of P1 and P2 (picture B and C) seem to have less dendritic connections compared to the healthy control (picture A), and they seem to be less nicely aligned. The reasons for this will be evaluated in the discussion.

DM1 disease markers in iNeurons.

We performed immunocytochemistry on iNeurons on DIV49 to check for DM1 disease markers. The results are shown in Figure 11. In line with our expectations, the iNeurons of the healthy control C2 did not show foci. The same holds for P1, where we also did not find RNA foci in the iNeurons. This is in accordance with what has been found earlier in the iPSCs that P1 did not show any RNA foci (see Fig. 8 C and D). P2 shows RNA foci in the iNeurons stage, which corresponds with the iPSCs of P2

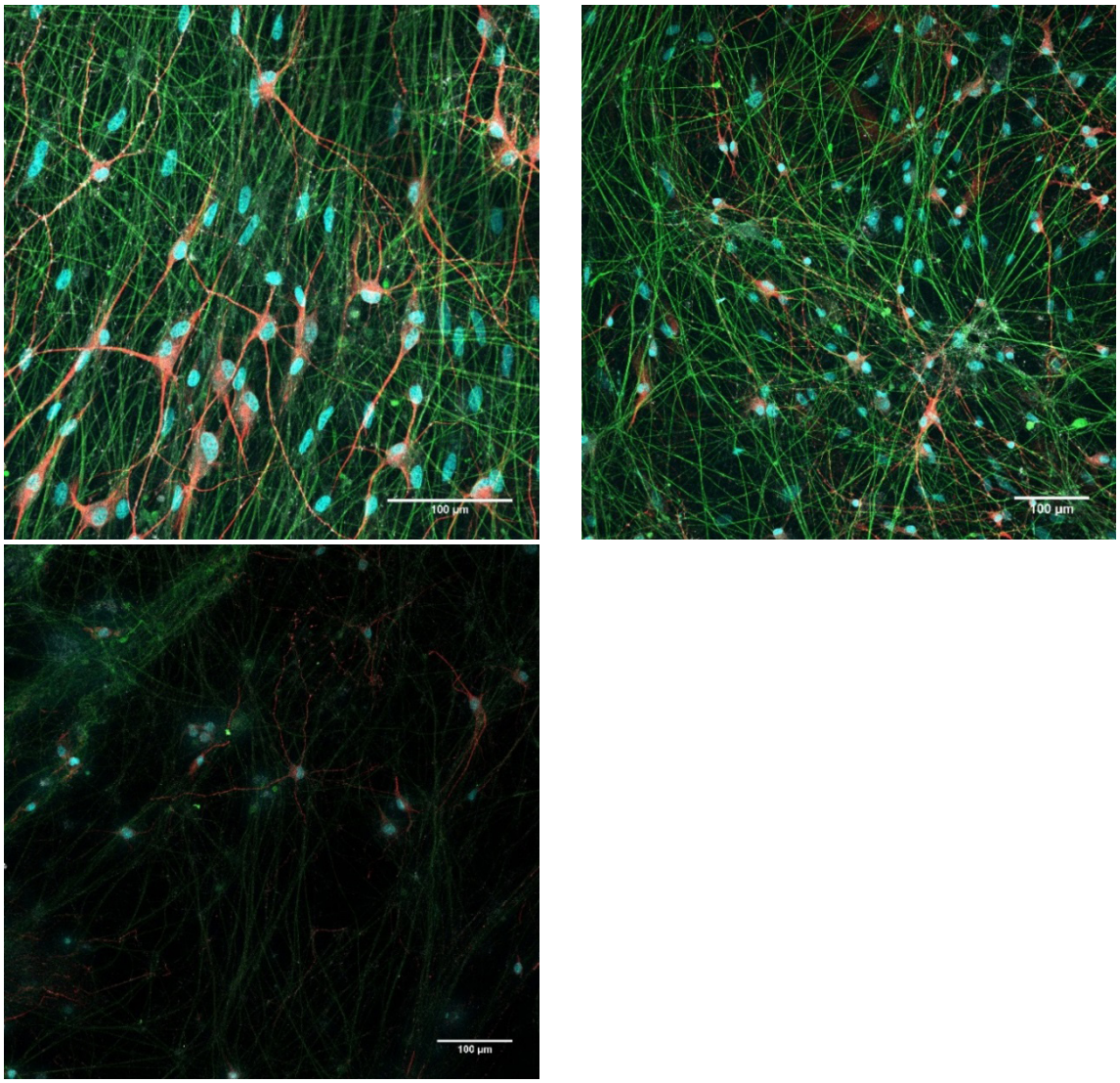

Figure 10. Immunocytochemistry of iNeurons from C2, P1 and P2 at DIV49 for neuron-specific markers. Image A shows iNeurons of C2, image B refers to P1 and image C shows the iNeurons of P2 with a zoom-in in greyscales of the (CAG)6 probe to better visualize RNA foci. The antibodies used are Pan-Axonal Neurofilament Marker (mouse monoclonal, BioLegend) in green for the axons, Microtubule-associated protein 2 (MAP2, rabbit polyclonal, Abcam) in red for the dendrites, Synapsin (guinea pig polyclonal, Synaptic systems) in grey for the synapses and Hoechst 33342 (10mg/mL solution in water, Invitrogen) in cyan for the nuclei. Images were acquired with a Zeiss LSM880 confocal microscope with 405 and 561 nm diode lasers, argon (458, 488, 514 nm) and a 633 nm laser using a x20 objective. The scale bar in the images indicates a length of 100µM.

showed foci previously (see Fig. 8 E).

Additionally, we performed a quantification of the number of foci per nucleus (Fig. 12). The results show that P1 had almost no foci, but P2 had up to 10 foci per nucleus, with an average of 1.6 foci.

Establishment of electrophysiological profile of iNeurons

For the analysis of the acquired electrophysiological data of the MEA test plate, we used the Multiwell-Analyzer software (multichannel* systems, MCS GmbH). The most important parameters for the characterization of neuronal activity are the mean percentage of random spikes, the mean burst rate (measured in bursts per minute), the mean network burst rate (measured in network bursts per minute) and the mean network burst duration (measured in milliseconds). A burst is defined as a minimum of 4 spikes in a short time frame. For a network burst, at least 6 electrode channels (per well) need to be

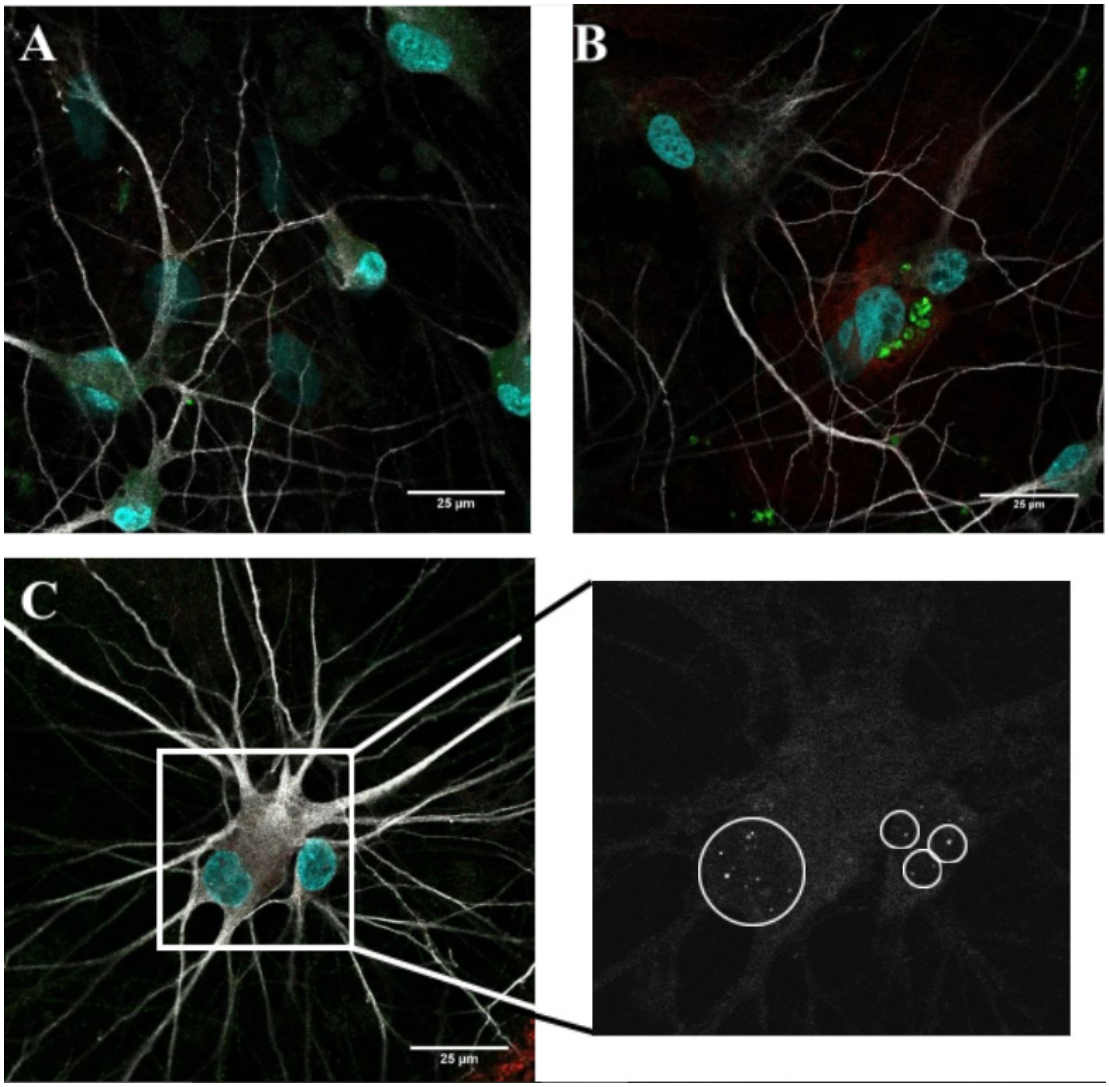

Figure 11. Immunocytochemistry of DM1 disease specific markers of iNeurons at DIV49 from C2, P1 and P2. A shows C2, B shows P1 and C shows P2. Stainings were performed for FISH (Stellaris) shown in red, MBNL1 shown in green, Hoechst 33342 (10mg/mL solution in water, Invitrogen) and Microtubule-associated protein 2 (MAP2, rabbit polyclonal, Abcam) shown in grey. MAP2 was added as a neuron-specific marker in order to separate the iNeurons from the rat astrocytes. Images were acquired with Zeiss LSM880 confocal microscope with 405 and 561 nm diode lasers, argon (458, 488, 514 nm) and a 633 nm laser using a x20 objective. The scale bar indicates a length of 25µM.

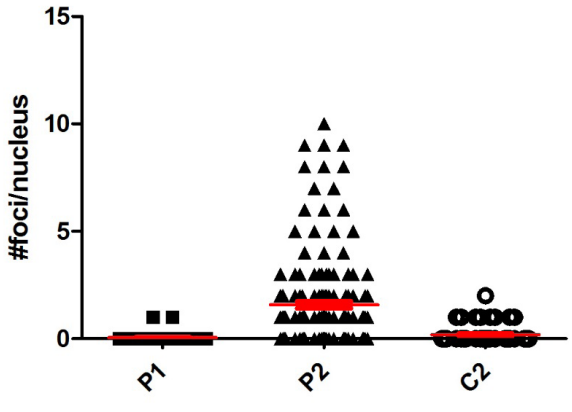

Figure 12. Quantification of RNA foci per nucleus. The quantification was performed on iNeurons at DIV49 from P1, P2 and C2, stained with DM1 disease specific markers. The number of RAN foci per nucleus were determined with FIJI (ImageJ). The red line indicates the mean, P1 = 0.05 foci/nucleus, P2 = 1.6 foci/nucleus, and C2 = 0.2 foci/nucleus.

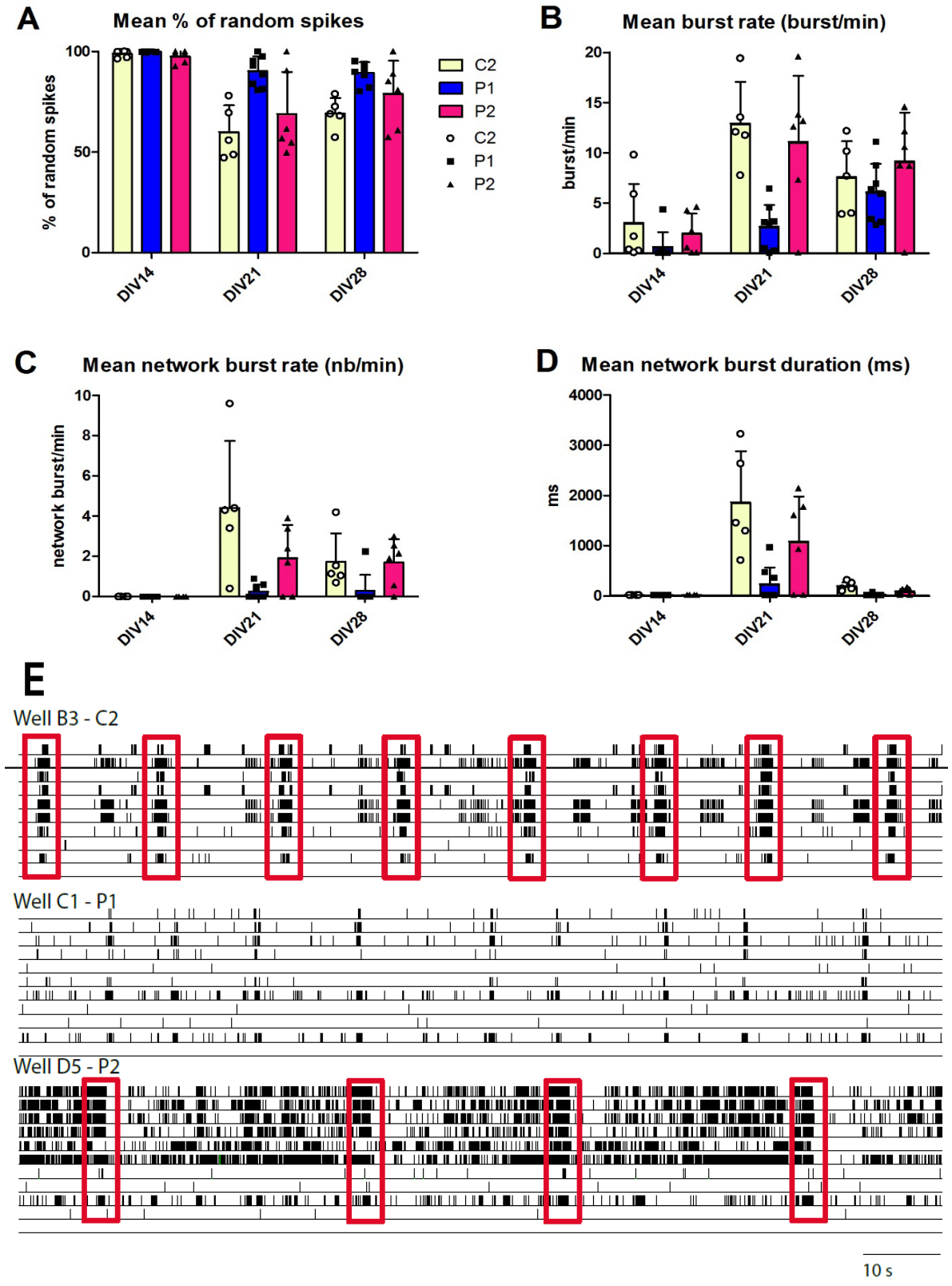

Figure 13. Electrophysiological profile of iNeurons from DIV14, DIV21 and DIV28. The included cell lines are of a control (referred to as C2), and two patients (P1 and P2). Graphs A-D show important parameters for analyzing the electrophysiological activity of neurons. Note: The data of DIV14 and DIV21 have been recorded with a sampling frequency of 20.000 Hz, whereas the data of DIV28 has been recorded with a sampling frequency of 10.000 Hz. Figure E shows a rasterplot of recorded activity on DIV28 with a length of 2 minutes. Three wells (B3, C1 and D5) are depicted, and each block refers to one cell line. In each block, every line refers to one electrode of this well. The network bursts are marked by the red boxes.

participating. The results are shown in Figure 13.

For these results, it is important that DIV14 and DIV21 should not be compared with DIV28 due to a different sampling frequency (DIV14 and DIV21: 20.000Hz and DIV28: 10.000Hz). The results of establishing an electrophysiological profile show that on DIV14, all three samples that were taken along show random spikes of roughly 100% (Fig. 13 A). Throughout differentiation, this behaviour changes the most in the control iNeurons (C2). Figure 13 B shows that the mean burst rate increased from DIV14 to DIV21, for all three samples. Figure 13 C and D show that on DIV14, the neurons are still too immature to form network bursts. However, from DIV21 on, the control iNeurons are able to form network bursts. It seems that the iNeurons of P2 are more able to form network bursts as well, even though we expected P1 to be more similar to the control. In the discussion section, some explanations for this will be provided.

Figure 13 E (on DIV28) gives a 2-minute overview of the electrophysiological recording of three distinct wells, one for each patient and the control. The topmost block shows the healthy control, with regular occurring network bursts. iNeurons of P1, depicted in the middle block, are not able to form network bursts. In the bottom row, the neuronal activity of P2 is shown and shows 4 network bursts in the 2 min time window. However, it also shows a lot of activity surrounding the network bursts. Possible reasons for this will be evaluated in the discussion.

Discussion

Repeat length of included samples

When we performed the Northern blot for a determination of the repeat length in P1 and P2, we only received inconclusive results, which is likely due to the very low gene expression level of DMPK. The results of the RT-qPCR of DM1 relevant genes show that DMPK is not highly expressed in iPSCs on RNA level.

The results of the TP-PCR show that the repeat of P1 grew a bit from 64-77 (in blood) to 87-97 (in iPSCs), due to somatic expansion (Du, Campau, Soragni, Jespersen, & Gottesfeld, 2013). This is completely in line with the results from immunofluorescence: P1 did not show any DM1 disease markers, such as RNA foci. The results of the TP-PCR for P2 show that the repeat in iPSCs is above 150, which was the same as in blood. Unfortunately, we do not know how long the repeat exactly is because the TP-PCR shows only up to a maximum of 650 bp. For P2 we expect the repeat to be relatively high because in both the iPSCs and the iNeurons of P2 we were able to find RNA foci. There is the possibility that the repeat has grown over time, due to somatic instability (Caillet-Boudin et al., 2014; Du et al., 2013; Morales et al., 2012; Yum et al., 2017). Du et al. (2013) found that the repeat expansion rate in iPSC is dependent on the length of the repeat, a longer repeat expands faster than a shorter repeat. But even a repeat of 50 expands over time. Another unknown variable is the repeat length of the samples in the iNeuron stage.

Differentiation of Tet-On 3G- & NGN2-positive iPSC lines into iNeurons

The differentiation of Tet-On 3G- and NGN2-positive iPSCs into iNeurons was successful. In the beginning we used three different cell densities to get the optimum and we were able to use the lowest cell density of 17,500 on a surface of 0.97 cm2. Unfortunately, in our differentiations the Ara-C seemed to be not as efficient as expected. On day five and six we were still able to see iPSCs in the neuronal culture (Fig. 6 and 7). This problem can possibly be solved by adding a higher concentration, such that all remaining iPSC will die off and can be washed away when the media is changed. Here, we used a concentration of 2 µM. Seibenhenner & Wooten (2012) report that Ara-C can be used up to a concentration of 5 µM, but that higher concentrations can have toxic effects on iNeurons.

Immunofluorescence and Immunocytochemistry

DM1 disease markers in iPSC

The results for the DM1 specific disease mar-

kers are in line with the expectations, such that P1 with a short repeat does not show any RNA foci but P2 with a longer repeat shows RNA foci. It is very likely for P1 that the threshold of the (CAG)6 probe is not reached and therefore no foci are visible, even though cells of P1 show a repeat (Jiang et al., 2004). For MBNL1 we did not get a signal (Fig. 8), which is also not surprising because when we tested the gene expression levels (Fig. 5) in the iPSCs of both patients we saw that MBNL1 is 10-fold lower expressed in the iPSCs (of P1 and P2) compared to in adult myoblasts. This can also be seen in 'The Human Protein Atlas' (https://www.proteinatlas.org/): MBNL1 shows very little expression in fibroblasts, same holds for MBNL2. MBNL3 is tissue-specific to female tissues, such as the placenta (Jiang et al., 2004). Han et al. (2013) also reported very low MBNL1 and MBNL2 mRNA levels in iPSCs.

iNeuron characterization

We characterized the generated iNeurons on DIV6 and on DIV49. On DIV6, the iNeurons were very immature, however, axons and dendrites are present (Fig. 9) (Frega et al., 2017). Due to their immature state, after 6 days of differentiation no synapses were present. However, they do develop after 7-20 days in vitro (Cullen et al., 2010). We also see relatively few dendritic connections, compared to in later stages. Unfortunately, we see on some images a strong signal at some spots in the green channel, which is due to dust or dirt on the coverslips.

On DIV49, the iNeurons reached a very mature stage (Frega et al., 2017), therefore, we were able to get a signal for synapsin (Fig. 10). In this differentiation experiment up to DIV49, we took a control sample along C2, in order to have a good comparison to the disease samples. We see that the dendrites of C2 seem to be nicely aligned and quite dense. In comparison, the dendrites of P1 seem to be less dense and not that nicely aligned. Unfortunately, the coverslips with iNeurons of P2 show only very little signal because after the fixation step many cells let loose from the coverslips. This was due to the COVID-19 pandemic restrictions. During the hospital lockdown the iNeurons were stored for too long in 1x PBS. We were lucky that only very little was washed away for C2 and P1. The problem can be solved by storing the iNeurons in 1% PFA, which prevents very large parts of the iNeurons from letting loose.

DM1 disease markers in iNeurons

The results of the DM1 disease markers in iNeurons show, that RNA foci are present in P2, as expected, and absent in C2 and P1, which is also in line with what we saw earlier (see discussion 3.1). We also performed immunofluorescence for MBNL1, however, we did not get a reasonable signal. This is not really surprising because MBNL1 is not expressed in the brain (Charizanis et al., 2012; Goodwin et al., 2015). Therefore, it is logical that we did not see MBNL1 foci in the nuclei. It would have been better to use a MBNL2 antibody, because MBNL2 is supposed to be highly expressed in the brain (Charizanis et al., 2012; Goodwin et al., 2015); Ramon-Duaso et al., 2020). Jiang and colleagues (2004) report that MBNL1 and MBNL2 are, among the muscleblind-like RNA binding proteins the ones that are strongly forming intranuclear foci. Therefore, we expect to see intranuclear foci when including MBNL2 for immunofluorescence on iNeurons. When we performed the immunofluorescence for DM1 specific disease markers, we added the antibody MAP2, for dendrites, to get a distinction between iNeurons and astrocytes. This was done because DAPI stains the nuclei of rat astrocytes and nuclei of human iNeurons.

Furthermore, we performed a quantification of RNA foci in iNeurons from C2, P1 and P2 on DIV49. The results were as expected, P1 showed almost no foci, same as C2 (see discussion 3.1). iNeurons of P2 showed up to 11 foci per nucleus which is also in line with previous results from immunofluorescence in iPSC. We know that in iPSC P2 has a repeat above 150, and we saw up to 11 RNA foci per nucleus, therefore, we would expect the repeat to be relatively long. However, this needs to be validated first by SP-PCR performed in iPSC and in iNeurons of P2. SP-PCR amplifies small amount of DNA molecules which are then detected by Southern blots (Dandelot & Gourdon, 2018; Yum et al., 2017). This technique has a broader detection range compared to the TP-PCR (Leferink et al., 2019).

Establishment of Electrophysiological profile in iNeurons

On DIV14, DIV21 and DIV 28 we performed electrophysiological recordings of iNeurons of C2, P1 and P2. The rasterplot of P2 shows a lot more activity than C2, we expected P2 to show less activity and less network bursts compared to P1 and C2. However, the activity we saw looks more like an 'overcompensation'. Similar results were found in a study by Sicot et al. (2017). They found that DMSXL mice show hyperexcitability in Purkinje cells, and their results suggest that glutamate transporter 1 (GLT1) downregulation in several brain areas causes broad neuronal hyperexcitability (Sicot et al., 2017). However, this will need to be further validated in order to draw conclusions if this is the case as reported by Sicot and colleagues (2017).

The rasterplot of P1 was also surprising to us. P1 has only a short repeat, therefore we expected the rasterplot of P1 to look similar to C2. The pattern shown in Figure 13 E (Well C1 – P1), shows regular firing of the neurons, however, not enough channels are participating in order to define it as a network burst. One possible explanation for this might be that P1 had a lower cell density compared to C2 and P2. Another possibility is that in all the wells for every patient and control, the iNeurons were not evenly distributed along the electrodes. This is also the reason why not every channel shows activity.

To improve our current electrophysiological data, we need to use a new MEA plate. By this we can rule out coating problems and leaking wells.

When electrophysiological recordings are performed, it is always of high importance to have a control in the same MEA plate. However, there are also smaller differences between different types of controls. The control (C2) used in this experiment is the wild-type c (WTc) which is also used in the lab of Dr. Nael Nadif Kasri (Radboudumc). The analysis of the neuronal activity of C2 reveals that, unfortunately, it is not fully ideal. On the one hand, some parameter such as the burst rate (burst/min) on DIV28 is in line with how it is supposed to look like but on the other hand, parameters such as the burst duration (in seconds) is very far away from ideal (Frega et al., 2019). A reason for this might be the MEA plate which was not ideal.

Overall, we would highly recommend to repeat this experiment with the recently mentioned aspects to be taken into account. Additionally, when the recordings are made, they need to be recorded all with the same sampling frequency. In this case, the recording of DIV14 and DIV21 were made with a sampling frequency of 20,000 Hz and the recording of DIV28 was done with a sampling frequency of 10,000 Hz. The different sampling frequencies make it difficult to compare the samples at the different stages of days in vitro.

Future Perspectives

Several experiments need to be carried out in order to get a better picture about the cognitive deficits in DM1 patients. SP-PCR needs to be performed to get a more precise repeat length for P2, and the repeat length needs to be determined in iNeurons of P1 and P2. Next to it, RT-qPCR for the gene expression levels has to be performed in ns=3, including a statistical analysis. Besides this, iNeurons from patients and control need to be harvested for RNA to perform RT-qPCR for gene expression levels on these samples, such that assumptions about changes in gene expression levels from iPSC to iNeurons can be made. Furthermore, when performing immunofluorescence on iNeurons of P1 and P2, the antibody for MBNL2 needs to be included instead of MBNL1 because of its higher expression in the brain (Charizanis et al., 2012; Goodwin et al., 2015). For better electrophysiological data, a new MEA plate needs to be used, and it is important that the iNeurons are spread equally among the electrodes and that each well has a similar cell density. The recordings need to be all at the same sampling frequency. Last but not least, experiments for alternative splicing need to be carried out for alternatively spliced genes which are regulated by MBNL2 (Table S1). When investigating alternative splicing, the CELF proteins should also be taken along because they also seem to be involved in the regulation of splicing mechanisms (Hernández-Hernández et al., 2013). With the

recently mentioned additional experiments, better conclusions can be drawn about the processes occurring in the DM1 brain.

Conclusion

The performed experiments show that we are able to differentiate iNeurons from iPSC from DM1 patients which show DM1 disease markers such as RNA foci. Additionally, we showed that the repeat in iPSC is expanding between passages. Unfortunately, we cannot draw conclusions about processes occurring and causing the DM1 brain phenotype. Concluding all experiments, we argue that our findings contribute to unravel the neuropathophysiology of DM1. However, to get the full spectrum, follow-up experiments for further validation need to be performed.

When we performed the immunofluorescence for DM1 specific disease markers, we added the antibody MAP2, for dendrites, to get a distinction between iNeurons and astrocytes. This was done because DAPI stains the nuclei of rat astrocytes and nuclei of human iNeurons.

Furthermore, we performed a quantification of RNA foci in iNeurons from C2, P1 and P2 on DIV49. The results were as expected, P1 showed almost no foci, same as C2 (see discussion 3.1). iNeurons of P2 showed up to 11 foci per nucleus which is also in line with previous results from immunofluorescence in iPSC. We know that in iPSC P2 has a repeat above 150, and we saw up to 11 RNA foci per nucleus, therefore, we would expect the repeat to be relatively long. However, this needs to be validated first by SP-PCR performed in iPSC and in iNeurons of P2. SP-PCR amplifies small amount of DNA molecules which are then detected by Southern blots (Dandelot & Gourdon, 2018; Yum et al., 2017). This technique has a broader detection range compared to the TP-PCR (Leferink et al., 2019).

References

André, L.M., van Cruchten, R.T.P., Willemse, M., & Wansink, D.G. (2019). (CTG)n repeat-mediated dysregulation of MBNL1 and MBNL2 expression during myogenesis in DM1 occurs already at the myoblast stage. *PLoS ONE, 14*(5), e0217317.

Beer, J.G., & Ochsner, K.N. (2006). Social cognition: A multi-level analysis. *Brain Research, 1079*, 98-105.

Braz, S.O., Acquaire, J., Gourdon, G., & Gomes-Pereira, M. (2018). Of Mice and Men: Advances of Neuromuscular Aspects of Myotonic Dystrophy. *Frontiers in Neurology, 9*, 74-93.

Caillet-Boudin, M.L., Fernandez-Gomez, F.J., Tran, H., Dahenens, C.M., Buée, L., & Sergeant, N. (2014). Brain pathology in myotonic dystrophy: when tauopathy meets spliceopathy and RNAopathy. *Frontiers in Molecular Neuroscience, 6*, Article 57.

Charizanis, K., Lee, K.-Y., Batra, R., Goodwin, M., Zhang, C., Yuan, Y., Shiue, L., Cline, M., Scotti, M.M., Xia, G., Kumar, A., Ashizawa, T., Clark, H.B., Kimura, T., Takahashi, M.P., Fujimura, H., Jinnai, K., Yoshikawa, H., Gomes-Pereira, M., Gourdon, G., Sakai, N., Nishino, S., Foster, T.C., Ares Jr., M., Darnell, R.B., & Swanson, M.S. (2012). Muscleblind-like 2-Mediated Alternative Splicing in the Developing Brain and Dysregulation in Myotonic Dystrophy, *Neuron, 75*, 437-450.

Cullen, D.K., Gilroy, M., Irons, H.R., & La Placa, M.C. (2010). Synapse-to-neuron ratio is inversely related to neuronal density in mature neuronal cultures. *Brain Research, 1359*, 44-55.

Dandelot, E., & Gourdon, G. (2018). The flash-small-pool PCR: how to transform blotting and numerous hybridization steps into a simple denatured PCR. *Bio Techniques, 64*.

Dhaenens, C.M., Schraen-Maschke, S., Tran, H., Vingtdeux,V., Ghanem,D., Leroy, O., Delplanque, J., van Brussels, E., Delacourte, A., Vermersch,P., Maurage, C.A., Gruffat, H., Sergeant, A., Mahdevan, M.S., Ishiura, S., Buée, L., Cooper, T.A., Caillet-Boudin, M.L., Charlet-Berguerand, N., Sablonnière,B., & Sergeant, N. (2008). Overexpression of MBNL1 fetal isoforms and modified splicing of Tau in the DM1 brain: Two individual consequences of CUG trinucleotide repeats. *Experimental Neurology, 201*, 467-478.

Dhaenens, C.M., Tran, H., Frandemiche, M.-L., Carpentier, C., Schraen-Maschke, S., Sistiaga, A., Goicoechea, M., Eddarkaoui, S., van Brussels, E., Obriot, H., Labudeck, A., Gevaert, M.H., Fernandez-Gomez, F.,

Charlet-Berguerand, N., Deramecourt, V., Maurage, C.A., Buée, L., Lopez de Munain, A., Sablonnière, B., Caillet-boudin, M.L., & Sergeant, N. (2011). Mis-splicing of Tau exon 10 in myotonic dystrophy type 1 is reproduced by overexpression of CELF2 but not by MBNL1 silencing. *Biochimica et Biophysica Acta, 1812*, 732-742.

Du, J., Campau, E., Soragni, E., Jespersen, C.M., & Gottesfeld, J.M. (2013). Length-dependent CTG-CAG triplet-repeat expansion in myotonic dystrophy patient-derived induced pluripotent stem cells. *Human Molecular Genetics, 22*(25), 5276-5287.

Elegheert, J., Behiels, E., Bishop, B., Scott, S., Woolley, R.E., Griffiths, S.C., Byrne, E.F.X., Chang, V.T., Stuart, D.I., Jones, E.J., Siebold, C., & Aricescu, A.R. (2018). Lentiviral transduction of mammalian cells for fast, scalable and high-level production of soluble and membrane proteins. *Nature Protocols, 13*, 2991-3017.

Frega, M., van Gestel, S.H.C., Linda, K., van der Raadt, J., Keller, J., van Rhijn, J.R., Schubert, D., Albers, C.A., & Nadif Kasri, N. (2017). Rapid Neuronal Differentiation of Induced Pluripotent Stem Cells for Measuring Network Activity on Micro-electrode Arrays. *J. Vis. Exp., 119*, e54900.

Frega, M., Linda, K., Keller, J.M., Gümüs-Akay, G., Mossink, B., van Rhijn, J.-R., Negwer, M., Gunnewick, T.K., Foreman, K., Kompier, N., Schoenmaker, C., van den Akker, W., van der. Werf, I., Oudakker, A., Zhou, H., Kleefstra, T., Schubert, D., van Bokhoven, H., & Nadif Kasri, N. (2019). *Nature Communications, 10*.

Gallo, J.-M., & Spickett, C. (2010). The role of CELF proteins in neurological disorders. *RNABiology, 7*(4), 474-479.

Gomes-Pereira, M., Bidichandani, S.I., & Monckton, D.G. (2004). Analysis of Unstable Triplet Repeats Using Small-Pool Polymerase Chain Reaction. In Kohwi, Y. (eds) Trinucleotide Repeat Protocols. *Methods in Molecular Biology™, 277,* 61-76.

Gomes-Pereira, M., Foiry, L., Nicole, A., Huguet, A., Junien, C., Munnich, A., & Gourdon, G. (2007). CTG trinucleotide repeat 'big Jumps': Large expansion, Small Mice. *PLoS Genetics. 3*(4): e52.

Goodwin, M., Mohan, A., Batra, R., Lee, K.-Y., Charizanis, K., Fernandéz Gómez, F.J., Eddarkaoui, S., Sergeant, N., Buée, L., Kimura, T., Clark, H.B., Dalton, J., Takamura, K., Weyn-Vanhentenryck, S., Zhang, C., Reid, T., Ranum, L.P.W., Day, J.W., & Swanson, M.S. (2015). MBNL Sequestration by Toxic RNAs and RNA Mis-Processing in the Myotonic Dystrophy Brain. *Cell Reports, 12*(7), 1159-1168.

Hamilton, M.J., McLean, J., Cumming, S., Ballantyne, B., McGhie, J., Jampana, R., Longman, C., Evans, J.J., Monckton, D.G., & Farrugia, M.E. (2018). Outcome Measures for Central Nervous System Evaluation in Myotonic Dystrophy Type 1 May Be Confounded by Deficits in Motor Function or Insight. *Froniers in Neurology, 9*(780).

Han, H., Irimia, M., Ross, P.J., Sung, H.-K., Alipanahi, B., David, L., Golipour, A., Gabut, M., Michael, I.P., Nachmann, E.N., Wang, E., Trcka, D., Thompson, T., O#Hanlon, D., Slobodeniuc, V., Barbosa-Morais, N.L., Burge, C.B., Moffat, J., Frey, B.J., Nagy, A., Ellis, J., Wrana, J.L., & Blencowe, B.J. (2013). MBNL proteins repress embryonic stem cell-specific alternative splicing and reprogramming. *Nature, 498,* 241-245.

Hernández-Hernández, O., Guiraud-Dogan, C., Sicot, G., Huguet, A., Luilier, S., Steidl, E., Saenger, S., Maciniak, E., Obriot, H., Chevarin, C., Nicole, A., Revillod, L., Charizanis, K., Lee, K.-Y., Suzuki, Y., Kimura, T., Matsuura, T., Cisneros, B., Swanson, M.S., Trovero, F., Buisson, B., Bizoy,J.-C., Hamon, M., Humez, S., Bassez, G., Metzger, F., Buée, L., Munnich, A., Sergeant, N., Gourdon, G., & Gomes-Pereira, M. (2013). Myotonic dystrophy CTG expansion affects synaptic vesicle proteins, neurotransmission and mouse behaviour. *Brain, 136,* 957-970.

Hernández-Hernández, O., Sicot, G., Dinca, D.M., Huguet, A., Nicole, A., Buée, L., Munnich, A., Sergeant, N., Gourdon, G., & Gomes-Pereira, M. (2013). Synaptic protein dysregulation in myotonic dystrophy type 1. *Rare Diseases, 1*(1).

Jiang, H., Mankodi, A., Swanson, M.S., Moxley, R.T., & Thornton, C.A. (2004). Myotonic dystrophy type 1 is associated with nuclear foci of mutant RNA, sequestration of muscleblind proteins and deregulated alternative splicing in neurons. *Human Molecular Genetics, 13*(24), 3079-3088.

Jinnai, K., Mitani, M., Futamura, N., Kawamoto,

K., Funakawa, I., & Itoh, K. (2013). Somatic instability of CTG repeats in the cerebellum of myotonic dystrophy type 1. *Muscle Nerve, 48*, 105-108.

Leferink, M., Wong, D.P.W., Cai, S., Yeo, M., Ho, J., Lian, M., Kamsteeg, E-J., Chong, S.S., Haer-Wigman, L., & Guan, M. (2019). Robust and accurate detection and sizing of repeats within the DMPK gene using a novel TP-PCR test. *Scientific Reports, 8*(8280).

Longman, C. (2006). Myotonic Dystrophy. *Journal of the Royal College of Physicians of Edinburgh, 36,* 51-55.

Morales, F., Couto, J.M., Higham, C.F., Hogg, G., Cuenca, P., Braida, C., Wilson, R.H., Adam, B., del Valle, G., Brian, R., Sittenfeld, M., Ashizawa, T., Wilcox, A., Wilcox, D.E., & Monckton, D.G. (2012). Somatic instability of the expanded CTG triplet repeat in myotonic dystrophy type 1 is a heritable quantitative trait and modifier of disease severity. *Human Molecular Genetics, 21*(16), 3558-3567.

Nakamori, M., & Takahashi, M.P. (2016). Myotonic Dystrophy. In Takeda, S., Miyagoe-Suzuki, Y., & Mori-Yoshimura, M. (eds) *Translational Research in Muscular Dystrophy*, 39-61.

Ramon-Duaso, C., Rodríguez-Morató, J., Selma-Soriano, E., Fernández-Avilés, C., Artero, R., de la Torre, R., Pozo, Ó.J., & Robledo, P. (2020). Protective effects of mirtazapine in mice lacking the Mbnl2 gene in forebrain glutamatergic neurons: Relevance for myotonic dystrophy 1. *Neuropharmacology, 170*.

Sanderson, M.J., Smith, I., Parker, L., & Bootman, M.D. (2014). Fluorescence microscopy. *Cold Spring Harbor protocols, 10,* pdb.top071795.

Scott, J.G., & Schoenberg, M.R. (2011). Deficits in Visuospatial/Visuoconstructional Skills and Motor Praxis. In Schoenberg M., Scott J. (eds) The Little Black Book of Neuropsychology. *Springer*, Boston, MA.

Seibenhenner, M.L., & Wooten, M.W. (2012). Isolation and Culture of Hippocampal Neurons from Prenatal Mice. *Journal of Visualized Experiments, 65*.

Settin, A., Elsobky, E., Hammad, A., & Al-Erany, A. (2008). Rapid Sex Determination Using PCR Technique Compared to Classic Cytogenetics. International *Journal of Health Sciences, 2*(1), 49-52.

Sicot, G., Servais, L., Dinca, D.M., Leroy, A., Prigogine, C., Media, F., Braz, S.O., Huguet-Lachon, A., Chhuon, C., Nicole, A., Gueriba, N., Oliviera, R., Dan, B., Furling, D., Swanson, M.S., Guerrera, I.C., Cheron, G., Gourdon, G., & Gomes-Pereira, M. (2017). Downregulation of the Glial GLT1 Glutamate Transporter and Purkinje Cell Dysfunction in a Mouse Model of Myotonic Dystrophy. *Cell Reports, 19*(13), 2718-2729.

Suenaga, K., Lee, K.-Y., Nakamori, M., Tatsumi, Y., Takahashi, M.P., Fujimura, H., Jinnai, K., Yoshikawa, H., Du, H., Ares Jr., M., Swanson, M.S., & Kimura, T. (2012). Muscleblind-Like 1 Knockout Mice Reveal Novel Splicing Defects in the Myotonic Dystrophy Brain. *PLoS ONE, 7*(3), e33218.

Udd, B., & Krahe, R. (2012). The myotonic dystrophies: molecular, clinical, and therapeutic challenges. *Lancet Neurology, 10*, 891-905.

Van der Plas, E., Hamilton, M.J., Miller, J.N., Koscik, T.R., Long, J.D., Cumming, S., Povilaikaite, J., Farrugia, M.E., McLean, J., Jampana, R., Magnotta, V.A., Gutmann, L., Monckton, D.G., & Nopulos, P.C. (2019). Brain Structural Features of Myotonic Dystrophy Type 1 and their Relationship with CTG Repeats. *Journal of Neuromuscular Diseases, 6*(3), 321-332.

Wenninger, S., Montagnese, F., & Schoser, B. (2018). Core Clinical Phenotypes in Myotonic Dystrophies. *Frontiers in Neurology, 9*, 7-15.

Yum, K., Wang, E.T., & Kalsotra, A. (2017). Myotonic dystrophy: disease repeat range, penetrance, age of onset, and relationship between repeat size and phenotypes. *Current opinions in genetics & development, 40,* 30-37.

Supplementary materials

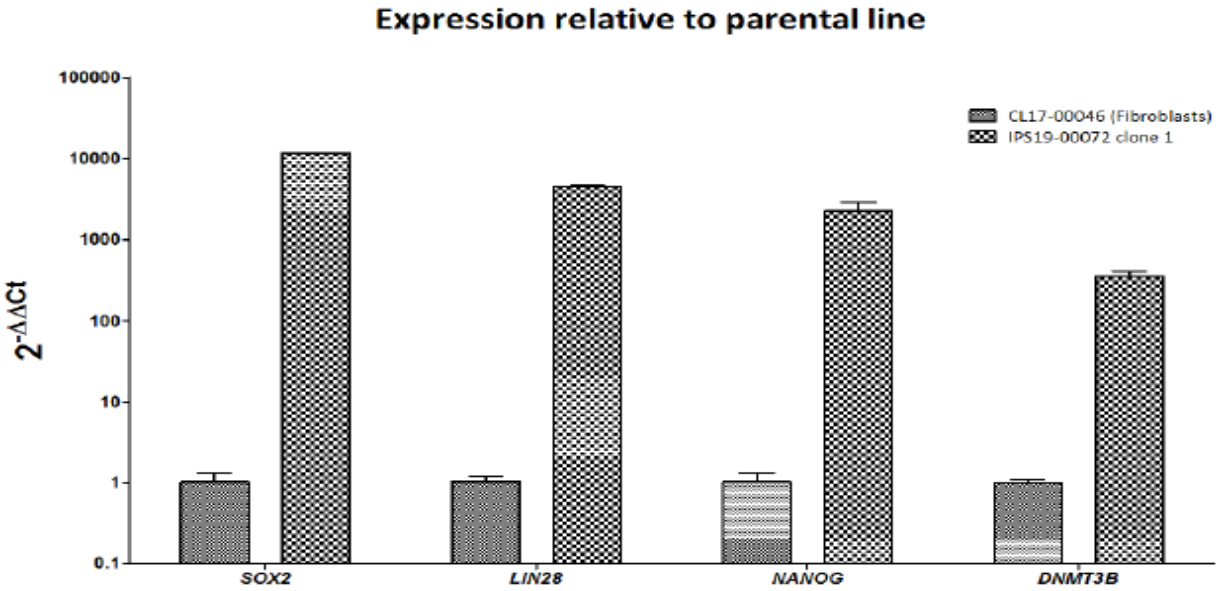

Figure S1. Gene expression relative to parental fibroblast line of P1. Pluripotency gene upregulation after reprogramming (ΔΔCt). The expression fold difference of the iPSCs is relative to parental fibroblasts.

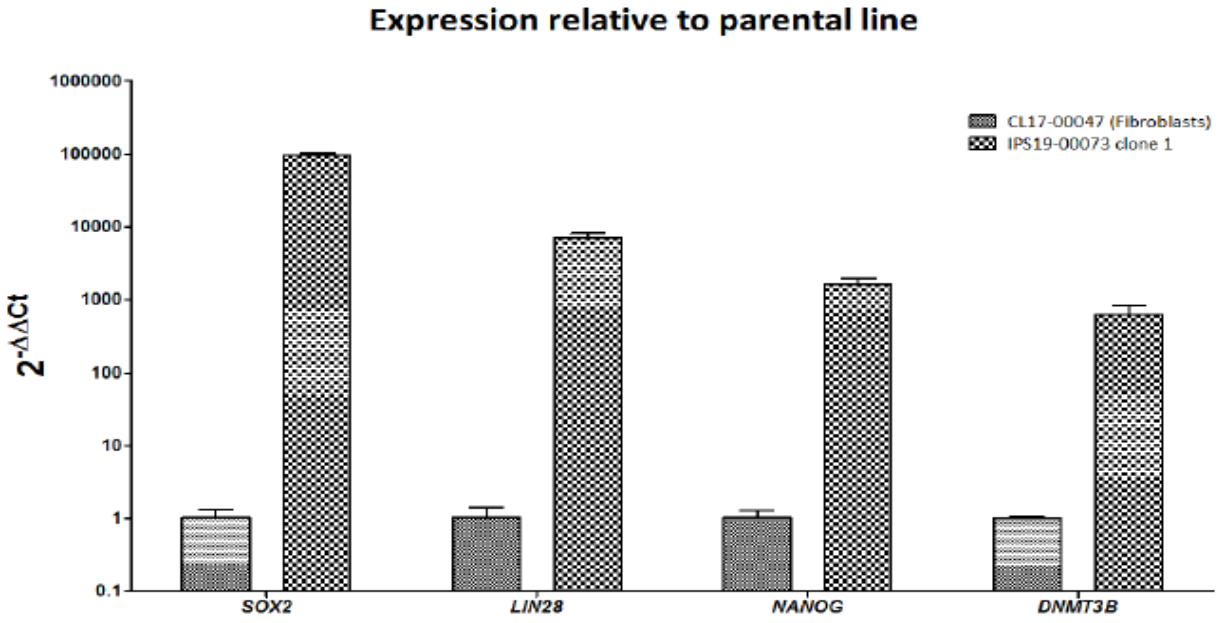

Figure S2. Gene expression relative to parental fibroblast line of P2. Pluripotency gene upregulation after reprogramming (ΔΔCt). The expression fold difference of the iPSCs is relative to parental fibroblasts.

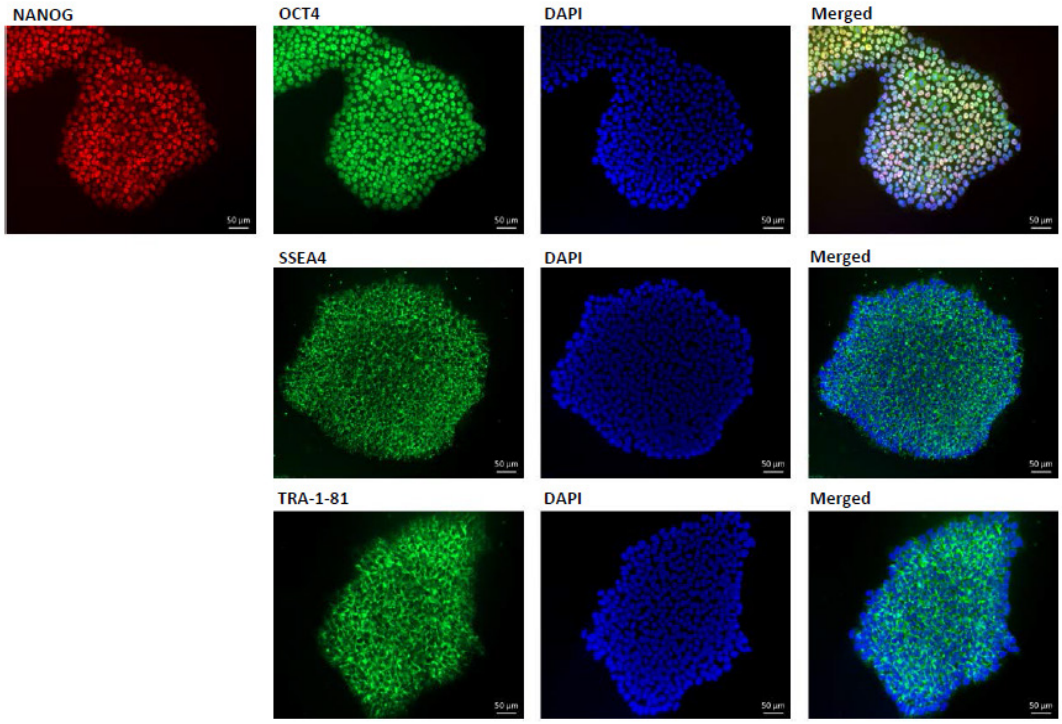

Figure S3. Immunofluorescence staining of the iPSC clone of P1 with pluripotency markers.

Table S1. List of alternatively spliced Genes in the Adult Brain, regulated by MBNL2.

Gene	Exon
Tanc2	E23a
Kcnma1	E25a
Limch1	E9
Spna2	E23
St3gal3	E3
Ndrg4	E14
Csnk1d	E9
Ppp1r12a	E14
Cacna1d	E12a
Add1	E15
Dlg2	E17b
Grin1	E5

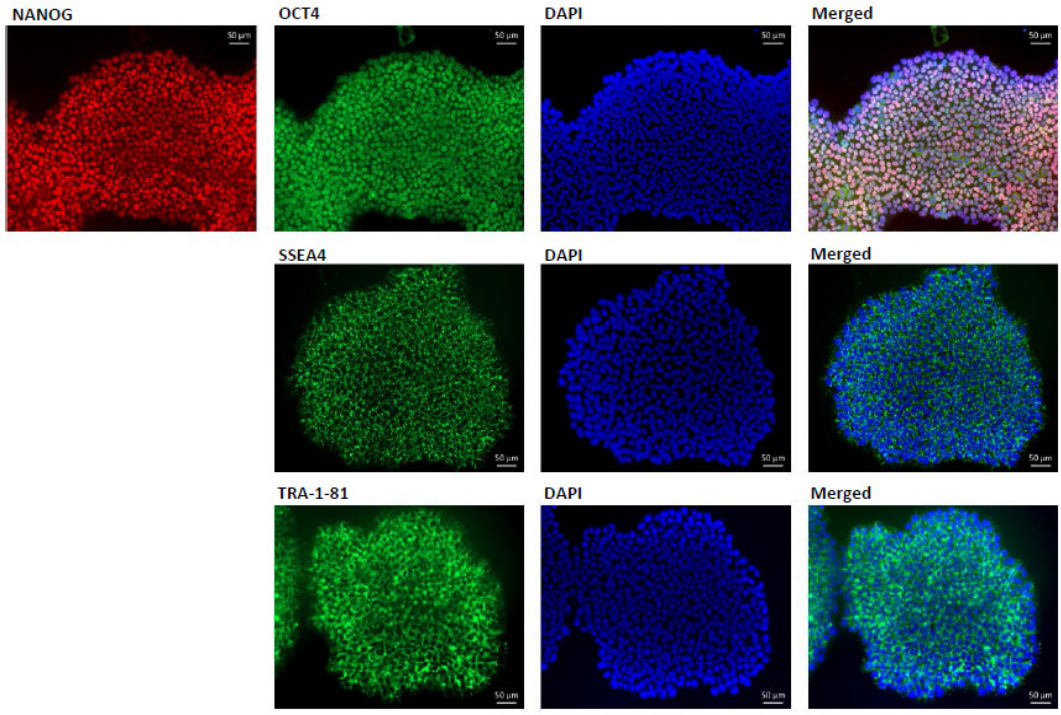

Figure S4. Immunofluorescence staining of the iPSC clone of P2 with pluripotency markers.

Table S2. RT-qPCR Primer Sequences. List of forward and reverse primer sequences used for assessment of gene expression levels in fibroblast derived-, pericyte derived iPSC and adult myoblasts.

Gene	Forward Sequence	Reverse Sequence
MBNL1 e2-4	5′- TAT GTC GAG AGT ACC AAC G -3′	5′- ACT GTG TTG TCA TTG GTG T -3′
MBNL2 e3-4	5′- CAG GAC TGA CAA ACT GGA -3′	5′- TGT TGT CAC TTG TGT CGA T -3′
MBNL3 e2-3	5′- AAT ACA CCT GTT CTG ATT CC -3′	5′- CAG TTT ATC TGA ACG CAT C -3′
DMPK e1-2	5′- ACT GGC CCA GGA CAA GTA CG -3′	5′- CCT CCT TAA GCC TCA CCA CG -3′
DMPK e15 3′	5′- TGC CTG CTT ACT CGG GAA A -3′	5′- GAG CAG CGC AAG TGA GGA G -3′
GUSB e11	5′- CTC ATT TGG AAT TTT GCC GAT T -3′	5′- CCG AGT GAA GAT CCC CTT TTT A -3′
TBP e3	5′- CCA CTC ACA GAC TCT CAC AAC -3′	5′- CTG CGG TAC AAT CCC AGA ACT -3′
HPRT1 e7-9	5′- TGA CAG TGG CAA AAC AATG -3′	5′- GGT CCT TTT CAC CAG CAA GCT -3′
GAPDH e1	5′- CCC GCT TCG CTC TCT GCT CC -3′	5′- CCT TCC CCA TGG TT CTG AGC G -3′

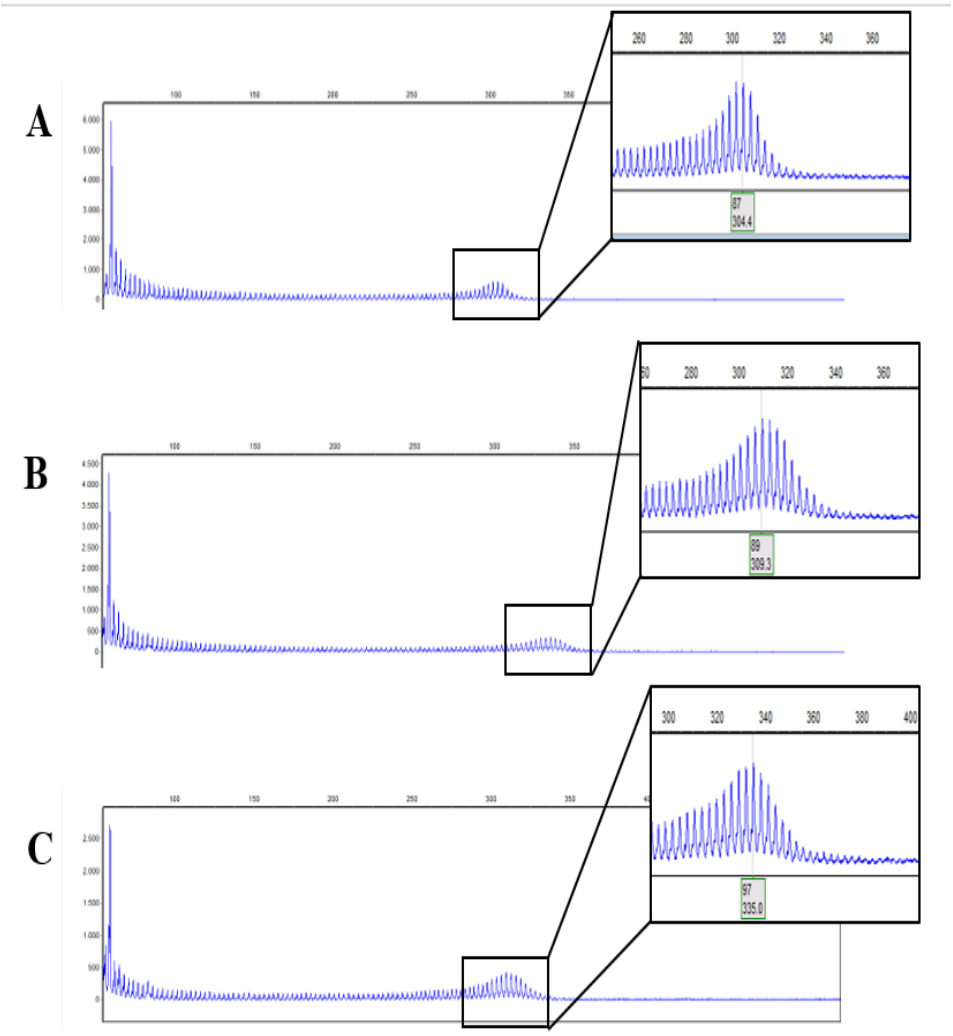

Figure S5. Electropherogram of TP-PCR of P1. A-C represent P1 at three different passage stages. A is passage 3, B is passage 16 and C is passage 9 of the iPSCs of P1 used to generate Tet-On 3G- & NGN2-positive cells. For A-C, the zoom in shows the repeat, which is for A: 87 repeats, for B: 89 repeats and for C: 97 repeats.

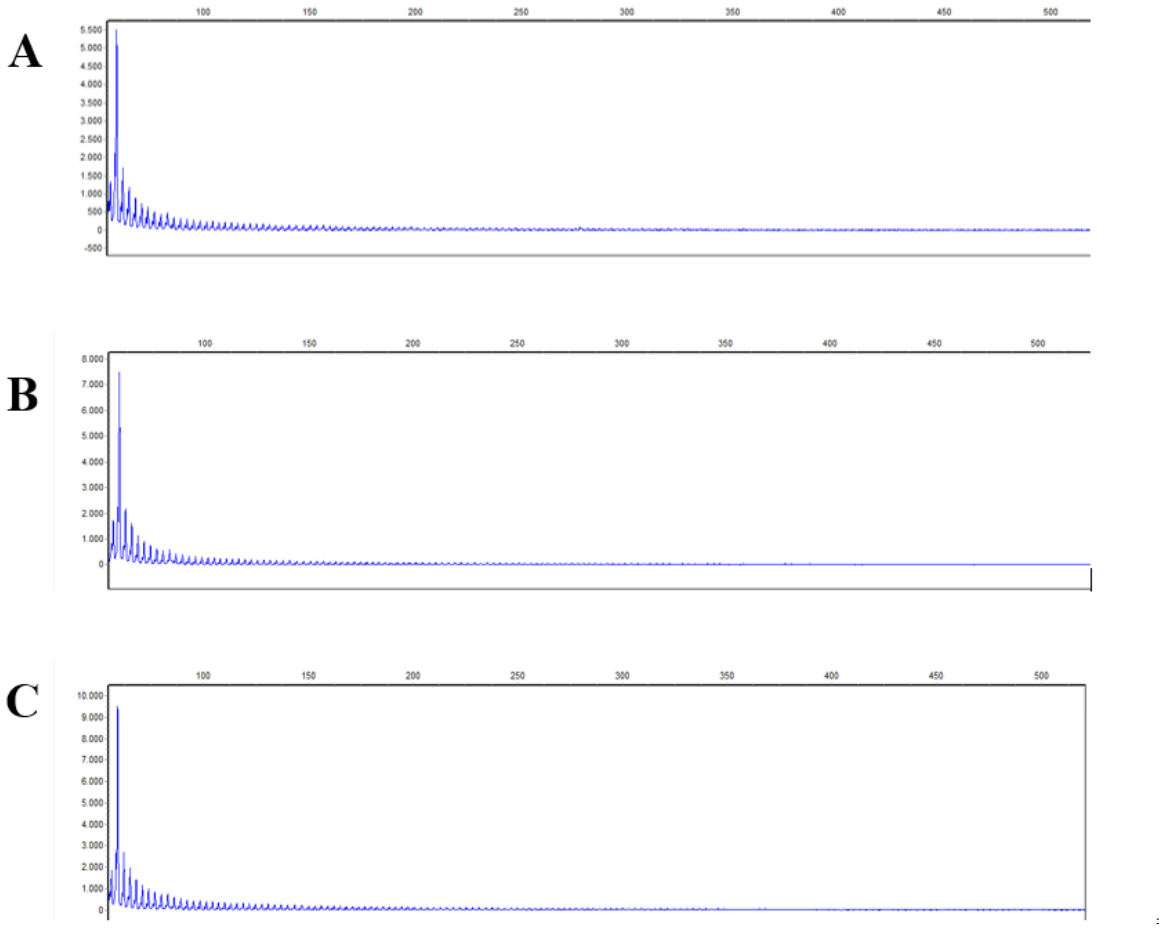

Figure S6. Electropherogram of TP-PCR of P2. A-C represent P2 at three different passage stages. A is passage 3, B is passage 11 and C is passage 9 of the iPSCs used to generate Tet-On 3G- & NGN2-positive cells. For A-C, the repeat is >150, a more precise determination is with TP-PCR not possible because every repeat above 150 is out of the determination range.

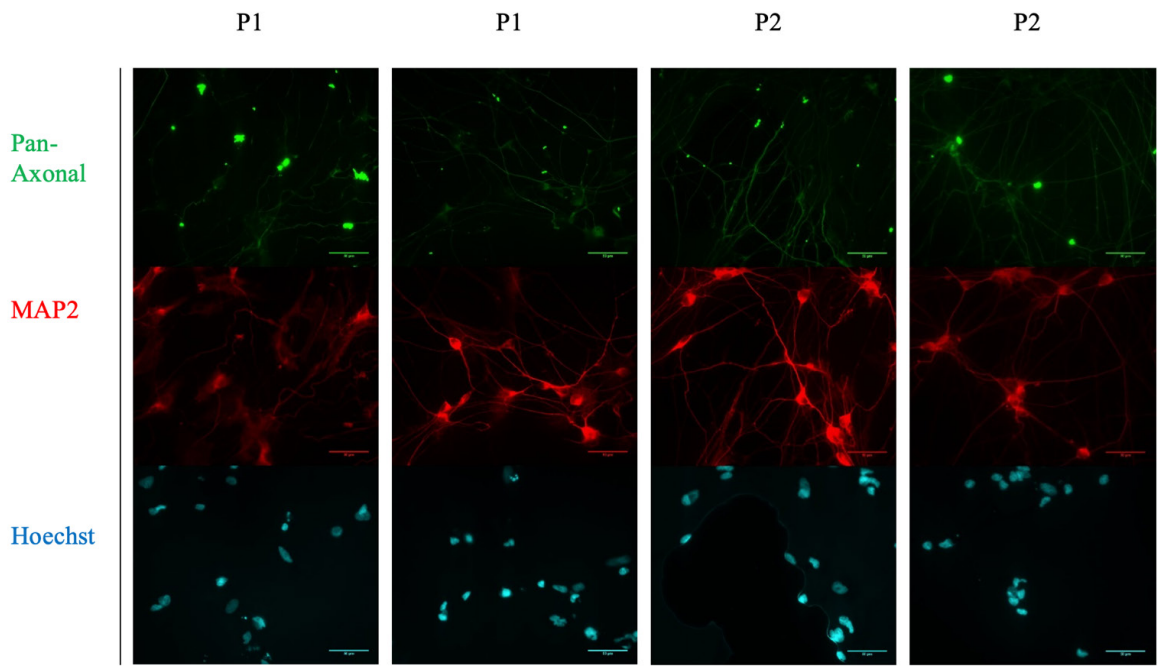

Figure S7. Immunocytochemistry of test-differentiated iNeurons at DIV6 from P1 and P2. Top row shows Pan-Axonal Neurofilament Marker (mouse monoclonal, BioLegend) in green, the second row shows Microtubule-associated protein 2 (MAP2, rabbit polyclonal, Abcam) in red, the third row shows Hoechst 33342 (10mg/mL solution in water, Invitrogen) in cyan. Images were acquired with a Zeiss Axio Imager Z1 microscope, using an x40 objective. The scale bar in the images indicates a length of 50 µM.

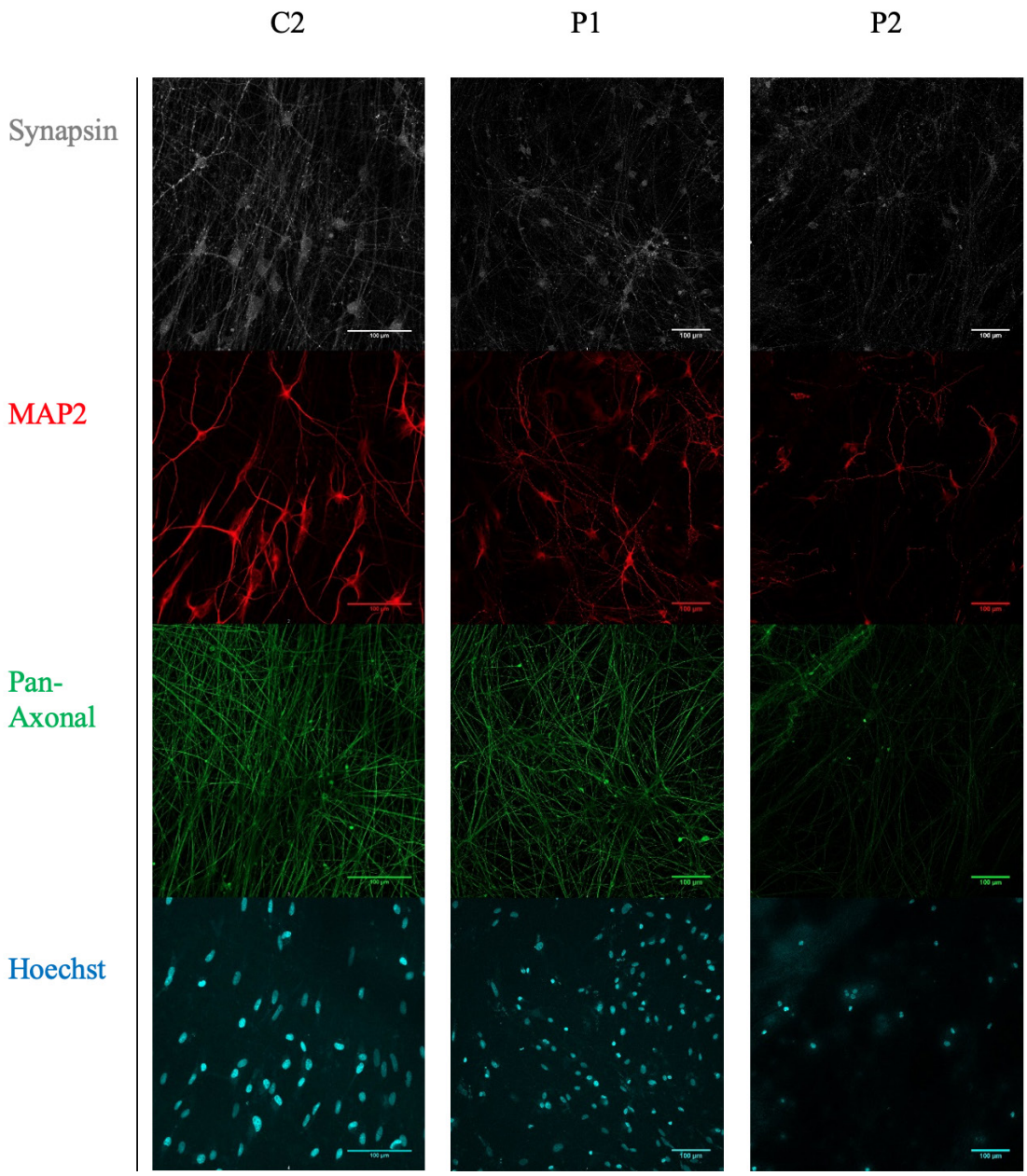

Figure S8. Immunocytochemistry of iNeurons at DIV49 from C2, P1 and P2. Top row shows Synapsin (Synapsin (guinea pig polyclonal, Synaptic systems) in grey for the synapses, the second row shows Microtubule-associated protein 2 (MAP2, rabbit polyclonal, Abcam) in red, the third row shows Pan-Axonal Neurofilament Marker (mouse monoclonal, BioLegend) in green and the bottom row shows Hoechst 33342 (10mg/mL solution in water, Invitrogen) in cyan. Images were acquired with a Zeiss LSM880 confocal microscope with 405 and 561 nm diode lasers, argon (458, 488, 514 nm) and a 633 nm laser using a x20 objective. The scale bar in the images indicates a length of 100µM.